Dynamic Periodic Event-triggered Multi-agent Consensus Using Relative-state Measurements: A Hybrid System Approach

by

Jiang Lin Li

A thesis submitted in partial fulfillment of the requirements for the degree of

Master of Science

in

Control Systems

Department of Electrical and Computer Engineering
University of Alberta

©Jiang Lin Li 2024

Abstract

Driven by technological advances in emerging fields such as autonomous vehicles, robots, and industrial internet-of-things, multi-agent systems (MASs) continue to be a prominent research area within Control Systems. Often, in practical applications, the agents employ information obtained from sensors, on-board and/or off-board, to accomplish complex tasks, asynchronously. Moreover, given the wide accessibility to electronic hardware and infrastructure, modern agents generally employ digital sensors and processors and coordinate wirelessly. The agents may even operate under a power storage device to allow for remote deployment. For modern agents, it is essential to emphasize that resources are often limited and access to information for control updates are only available when sampled. Given these potential resource constraints, there is significant interest in further studying control protocols, which incorporate the characteristics of digital hardware, to reduce resource consumption while still achieving the control objectives.

In this thesis, two problem formations are considered. Firstly, we consider the problem of distributed MAS consensus where the agents' dynamics follow a single-integrator. The control protocol of each agent employs local relative-state measurements, at their own sampling frequencies, and a dynamic periodic event-triggered protocol to dictate when control updates occur. Unlike continuous-time event-triggered protocols, the periodic event-triggered protocol only checks for events at discrete event-monitoring instants. Between sub-

sequent event-monitoring instants, the agents have no access to information regarding its neighbours. In our formulation, the event-monitoring instants are governed by sampling periods whose bounds are explicitly pre-computed, individually, for each agent. As a result, the designed control protocol is inherently asynchronous, even when the event-trigger mechanism is redundant, and avoids Zeno-behaviour by design. To unify the continuous-time agents' dynamics and both the discrete-time sensing and controller updates, the overall MAS is modelled and analyzed within the hybrid system framework.

Our second problem formulation aims to encompass a broader range of implementations. As such, we extend the agents' dynamics within the first problem formulation from a single-integrator to linear time-invariant systems. However, it is worth noting that since reaching consensus by stabilizing to the origin is trivial, we instead focus on achieving consensus to a new stabilizing set other than the origin. Furthermore, within our second problem formulation, we explore two constructions of the dynamic periodic event-triggered protocol, where the second construction is aimed at reducing the event frequency through incorporating an independently tunable term.

For both problem formulations, we prove consensus of the MAS utilizing the Lyapunov stability theorem within the hybrid system framework. We also provide sufficient conditions on the construction of the dynamic periodic event-trigger mechanisms and bound between event-monitoring instants such that consensus is guaranteed. Numerical examples, simulations, and comparisons are provided to demonstrate the utility and effectiveness of the results.

Preface

- Chapter 3 has been accepted as: Jiang Lin Li, Mani H. Dhullipalla, Tongwen Chen,"Periodic event-triggered consensus using relative-state measurements: a hybrid system approach", *Proc 26th International Symposium on Mathematical Theory of Networks and Systems*, August 19-23, 2024, Cambridge, UK.

Acknowledgements

After almost a decade of employment in industry and disconnected from the academic community, pursuing a master's degree in Control Systems proved challenging. The success of this pursuit of higher education, a rewarding experience, would not have been possible without all those who have supported me along the way.

First and foremost, I would like to express my deepest gratitude to my supervisor, Dr. Tongwen Chen, for introducing me to multi-agent systems and event-triggered control. It was a great privilege to have been afforded the opportunity to study under his guidance and learn from his expertise. His investment in his students and dedication to fostering an environment of academic curiosity has greatly shaped my academic and professional development, which will pay dividends throughout my career as an engineer.

Furthermore, I am forever grateful to Dr. Mani H. Dhullipalla for expanding my horizon to hybrid systems and the countless hours he dedicated to sharing his insights and engaging in discussions. I was truly inspired by his passion and relentless pursuit of knowledge, down-to-earth nature, and similar love for adventure. His mentorship significantly enriched my learning experience throughout the navigation of my academic program.

To all the group members of the CRC lab, I will never forget the inclusivity, bond, and advice that you've all extended to me. Your friendship made my time with the group truly enjoyable. It was a pleasure tackling the academic journey together, and I look forward to your future accomplishments.

I would like to acknowledge the Natural Sciences and Engineering Research Council of Canada (NSERC), the Faculty of Graduate Studies and Research

(FGSR), the Graduate Student Association (GSA), and the Department of National Defence (DND) for making this endeavour financially possible.

Lastly, I am grateful to my family for their unwavering support. To my beloved wife, Xiao Han, words cannot fully express my appreciation to you for your persistent mental support, encouragement, and affection.

Contents

List of Figures

List of Tables

List of Symbols

$\mathbb{R}^n$	Set of all real vectors of n-dimension ($n = 1$ when superscript omitted)
$\mathbb{N}^n$	Set of all integer-valued vectors of n-dimension ($n = 1$ when superscript omitted)
$\mathbb{R}^n_{\geq 0}$	Set of all non-negative real vectors of n-dimension ($n = 1$ when superscript omitted)
$\mathbb{N}^n_{\geq 0}$	Set of all non-negative integer-valued vectors of n-dimension ($n = 1$ when superscript omitted)
$\mathsf{diag}(v)$	Square diagonal matrix with elements of $v \in \mathbb{R}^n$ along the main diagonal
$\mathsf{blkdiag}(\{V\})$	Block diagonal matrix with elements of the sequence $V = \{V_1, \cdots, V_N\}$, where V_i are matrices, along the main diagonal
$\mathbf{1}_N$	Column vector of all ones of size N
$\mathbf{0}_N$	Column vector of all zeros of size N
$\tilde{\mathbf{0}}_i$	Column vector, of appropriate dimension, of zeros with 1 in the i-th element
$A_{N\times N}$	Matrix A of size $N \times N$
$\mathcal{I}_i$	$\mathsf{diag}([1, \cdots, 0, \cdots 1])$ with 0 at the $i-$th place
I_N	$N \times N$ identity matrix

$\otimes$	Kronecker product operator
$A \setminus B$	Set of elements in A that are not in the set $B \subseteq A$
$A \cup B$	Union of the sets A and B
$\|\cdot\|$	Euclidean norm of a vector or spectral norm of a matrix
$\|\cdot\|$	Absolute value of a scalar
∇	Gradient operator
$\emptyset$	Null set
$\langle \cdot, \cdot \rangle$	Dot product operator
$\Lambda_i(A)$	i-th eigenvalue of the square matrix A, where $\Lambda_1(A) \leq \cdots \leq \Lambda_N(A)$
$\Lambda_m(A)$	Minimum eigenvalue of the square matrix A
$\mathsf{dom}\, v$	The domain of v

List of Acronyms

AGT	Algebraic Graph Theory
ASM	Absolute-State Measurement
CPU	Central Processing Unit
CT	Continuous-Time
CTETM	Continuous-Time Event-Trigger Mechanism
DT	Discrete-Time
EMI	Event-Monitoring Instant
ETC	Event-Triggering Condition
ETM	Event-Trigger Mechanism
ISS	Input-to-State Stability
MAS	Multi-Agent System
MASP	Maximum Allowable Sampling Period
PETM	Periodic Event-Trigger Mechanism
RSM	Relative-State Measurement
UAV	Unmanned Aerial Vehicle

Chapter 1

Introduction

In this chapter, the motivation behind research involving multi-agent systems (MASs), in combination with the consensus problem, event-triggered control protocols, and the hybrid system framework are introduced. Next, a survey of existing literature addressing the aforementioned[1] are provided. Inspired by previous studies, the current research gaps are identified, thereby inviting further exploration. Finally, the specific contributions and a brief outline of this thesis are given.

1.1 Research Motivation

MASs can be characterised as a group of dynamic systems (agents) that coordinate, typically according to a communication topology, to cooperatively accomplish collective objectives that are often too complex for a single agent. General applications of MASs include, but are not limited to, cooperative robots [1], smart grids [2], coordination of spacecrafts [3], and intelligent traffic management [4]. Naturally, within MASs, one of the fundamental areas of research revolves around the problem of consensus, see articles [5], [6], [7], and [8]. Consensus, as defined in [9], can be described as all connected agents asymptotically converging to an agreement state(s) from any initial conditions. Some potential contemporary applications of consensus, as investigated in [10], include rendezvous, formation control, and axial alignment of unmanned aerial vehicles (UAVs), and sensor agreement, in the context of wireless sensor networks and sensor fusion. As can be seen by the spectrum of available

[1]Except for the hybrid system framework. The literature review of which will instead be consolidated within Chapter 2 - Preliminaries.

literature, the concept of MAS consensus has been historically well studied; however, emergence of new hardware and communication protocols introduce fresh implementation bottlenecks to this classical problem.

In practical applications, agents often employ information obtained from sensors, on-board and/or off-board, for control updates. With modern advancements and wide accessibility to electronic hardware and communication infrastructure, the agents in MASs increasingly become digital. Here within, we define the term "modern agents" to capture agents that possess one or more of the following components such as: digital sensors, which sample physical quantities in specified intervals; processors, which quickly perform computations using discrete values; digital transceivers, which enable high-bandwidth digital wireless communication; and potentially a power storage device, which allows for remote operations. In this way, modern agents have a greater capacity and degree-of-freedom, compared to hard-wired systems, for accomplishing tasks both distributively, where each agent is responsible for its own decision-making, and asynchronously, where each agent operates on its own clock for making decisions.

As sensing, computational, communication, and energy resources are finite, resource-constraint circumstances may arise as a result of design requirements (namely, deliberate extension of operation time for battery operated devices or reduction of actuator duty cycle [11]), or as a result of overloading (processor utilization saturation). In fact, for a UAV studied in [12], between 26-66% CPU utilization can be expected solely for the UAV's flight control. This emphasizes that control can draw significant computational resources and divert those resources away from being utilized for non-control task scheduling [13], such as image processing in support of surveillance operations. In such cases, there may be an interest to sacrifice a relatively small degree of control performance in order to save or divert resources to better support the overall mission.

One possible approach to overcoming the resource-constraint, in the context of control, is the implementation of an event-triggered protocol where control actions are only taken when specific conditions are met. Ideally, a well constructed event-trigger mechanism (ETM) eliminates computation and implementation of redundant control actions. Also, the ETM must avoid Zeno-behaviour, defined as an infeasible phenomenon where infinite events

occur within a finite time [14], from occurring. For modern agents, as access to continuous-time (CT) information is not only resource expensive but also unrealistic due to the characteristics of digital hardware (namely, sampling and discrete computation), this presents an additional layer of complexity in the design of the ETM such that the control objectives remain guaranteed.

As all physical systems in the real world exhibit CT behaviour, the integration of digital sensors, digital controllers, and an ETM within modern agents result in discrete-time (DT) control updates and may lead to nonlinear closed-loop dynamics. As a consequence, the rich dynamics of the closed-loop system is difficult to be modelled solely as a CT or DT system. A framework that unifies the CT dynamics of the physical agents with the DT control updates is necessary in order to better analytically study the control performance and trajectory of MASs comprising of modern agents.

1.2 Literature Survey

This thesis studies the MAS consensus problem, involving modern agents, and the design of ETMs that are realistic for implementation with digital hardware. The overall objective is to alleviate the impact of resource-constraint circumstances while guaranteeing consensus. In this section, we present a literature survey utilizing a building block approach of associated concepts. Specifically, we first present detailed literature reviews on multi-agent consensus, followed by various constructions of event-triggered protocols, and the approaches to avoid continuous monitoring of event-triggering conditions (ETCs). When appropriate, we draw implications from theory to real-world implementation.

1.2.1 Multi-agent Consensus

One of the main characteristics defining MASs is the coordination among agents; this implies that some form of communication topology exists. The communication topology[2] represents the protocol of information flow between agents. The algebraic graph theory (AGT) [15] effectively models the communication topology through the interconnection of nodes and edges. Within

[2]Sometimes also referred to as network or interaction topology depending on system structure.

MASs, most communication topologies can be captured by either directed or undirected graphs. In the former, as the name suggests, information flows one-way between at least one agent in the network to another connected agent. Meanwhile, in the latter, information flows bi-directionally between all connected agents. In the literature [16], the authors employed a directed graph while the authors of [17] employed an undirected graph. Under both graphs, the degree of connectivity has profound implications in terms of implementation. When more connections exist, it results in more information being exchanged; thus, more information available for control updates but at the cost of occupying greater bandwidth.

As previously mentioned, consensus is one of the fundamental problems in MAS research. From [18], consensus can be mathematically described as:

$$\lim_{t\to\infty} \|x_i(t) - x_j(t)\| = 0, \, \forall i, j \in \mathcal{V}, \tag{1.1}$$

where $x_i(t)$ denotes the state of agent i and $\mathcal{V}$ denotes the index set associated with the agents within the communication topology. It can be said that the consensus problem is solved if eq (1.1) is satisfied. However, in some cases, eq (1.1) is difficult to be satisfied; thus, a weaker condition is practical consensus defined as:

$$\lim_{t\to\infty} \|x_i(t) - x_j(t)\| \leq \Delta, \, \forall i, j \in \mathcal{V}, \tag{1.2}$$

where Δ is a positive value representing the upper bound on consensus performance. Generally, consensus can be guaranteed in the absence of quantization and disturbance, as seen in [19], while only practical consensus can be guaranteed when those considerations are involved, as seen in [20]. An important observation based on eq (1.1) is that stabilization to the origin, as studied in [21], also satisfies the condition for consensus. However, this is considered a trivial form of consensus. As such, the study of the consensus problem focuses on satisfying eq (1.1) at points other than the origin, as demonstrated in [22] by the unbounded state trajectories (typical in kinematics) but convergent consensus state trajectories.

In MAS consensus, information exchange between agents can occur by absolute-state measurements (ASMs), see [17] and [23], or by relative-state measurements (RSMs), see [24], [25], [19], and [26]. In the former approach, agents broadcast their states to neighbouring agents, which are then utilized to

update control. In the latter approach, agents having the capability through on-board sensors (e.g., radar, lidar devices, or computer vision) to directly obtain the relative states, such as distance, of neighbouring agents for control updates. The attraction in utilizing RSMs within MASs is that impact of network overloading and communication constraints, studied in [27], are largely mitigated as information exchange between agents are obtained directly by distributed local sensors rather than over the network. Given the advantages and readily available hardware to support implementation, it is of benefit to further study the MAS consensus problem utilizing RSM.

1.2.2 Event-triggered Protocols

As demonstrated in [28], the event-triggered protocol reduced control updates by 26% compared to the sample-data control protocol while obtaining similar system responses. By triggering events only when it is necessary, event-triggered protocols have the potential to reduce resource consumption and control actuation, thus alleviating the impacts of resource-constraint circumstances. When exactly events are triggered depends on not only the ETC but naturally when the ETC is checked, namely event-monitoring instants (EMIs).

[19] and [24] employed CT event-monitoring, or continuous-time event-triggered mechanism (CTETM). In this, the event conditions are monitored continuously and when the ETC is violated, an event is immediately triggered which prompts control to be updated. Meanwhile, [29], [30], and [31] employed periodic event-monitoring, or periodic ETM (PETM). Here, the event-conditions are checked only at discrete instants in time, either periodically or aperiodically, with event-monitoring being inactive in between subsequent EMIs. For PETMs, as events can only be triggered at these discrete EMIs, the inter-event time is always lower bounded by the event-monitoring interval. As a result, the inter-event time is always a positive value; thus, Zeno behaviour is avoided by construction. Studied in [32], combining the characteristics of CTETM and PETM lends to a time-regulation ETM. In time-regulation ETM, there is a period of inactivity where the ETC is not checked, behaving like a PETM, and after such inactivity period elapses the ETC is continuously checked, behaving like a CTETM. Each approach to event-monitoring possesses specific advantages but also implications. Based on simulations, in

terms of control performance and event-triggering frequencies when all else are equal, CTETM results in faster control performance with a reduced event frequency compared to PETM but at a greater sensing cost and potential for Zeno-behaviour. PETM has the advantage of conserving sensing resources but may incur more frequent events. Striking a balance between how often to check for events, event-triggering frequency, and system performance is sometimes a challenge [33]. Strategies to avoid continuous monitoring of event conditions is further investigated in depth within Subsection 1.2.3.

Vital to any ETM is the design of the ETC such that events are triggered only as needed, Zeno-behaviour is avoided, and most importantly consensus, or potentially in the practical sense, remains guaranteed. In the literature, typically the ETC is a function taking arguments of some variable of the measurement error and a constant threshold [34], time-dependent threshold [20], state-dependant threshold [19], or dynamic threshold [35].

With a constant threshold ETC, an event is triggered when the measurement error exceeds a constant threshold. Such an ETC is capable of completely avoiding Zeno-behaviour in linear MASs but may be unable to achieve strict consensus. This is due to the fact that for time $t > M \in \mathbb{R}_{\geq 0}$, the measurement error is small enough, but not zero, that it never exceeds the constant threshold. As a consequence, no events are triggered after time $t > M$, with which no control updates occur to bring the agents to consensus.

With time-dependant threshold ETC, a monotonically time-decaying function, usually a decaying exponential, replaces the constant threshold. By virtue of any time instant the time-decaying function is simply a constant threshold, Zeno-behaviour is avoided, and as time approaches infinity, the threshold converges to zero. Therefore, achieving consensus is possible. However, the cost is that the lower bound of the inter-event times relies on time and the initial states [18], with possibility of more frequent events as time progresses if the rate of the error growth exceeds the rate of the decay of the threshold. It is worth mentioning that for both constant and time-dependant thresholds, due to the absence of feedback, the design parameters for these thresholds can be independently selected to influence the consensus performance and the event frequency.

State-dependent thresholds typically utilize the norm of the consensus error as the threshold, based on the input-to-state stable (ISS) condition. As a

result, the event frequency typically is more consistent due to feedback; Zeno behaviour is avoided; achieving consensus is possible in linear MASs.

For dynamic thresholds, typically a virtual auxiliary variable that possesses dynamics of its own is defined and utilized. The auxiliary variable takes agent information as input, facilitating feedback, to reduce the likeliness of events by considering the cumulative effects of the agents' trajectories. The ETC is then based on this dynamic auxiliary variable. With proper design, it is possible to achieve consensus, Zeno-free behaviour, and reduce the event-triggering frequency. However, with dynamic ETC, there exists a slight additional computational cost as a result of computing the evolution of the auxiliary variable. Nonetheless, with the advantages in reducing the event frequency, the dynamic ETC is a suitable candidate for implementation.

Lastly, the ETC within the ETM can be evaluated either centrally or distributively. In the former, the ETM and ETC are centrally monitored and when conditions are violated, then all agents in the network trigger an event in a synchronous manner [17]. To employ the centralized approach, it requires that each agent monitors the global error, which requires continuous communication with either a central node or access to the states of all other agents in the network. In the distributed approach, each agent monitors its own ETC and triggers events independently of event-triggering of connected agents, thus often resulting in asynchronous control updates between agents. As modern agents have the capability to perform local computations and updates, paired with the impracticality of obtaining global information, the distributed approach encompasses greater breadth of real-world implementations.

1.2.3 Avoiding Continuous Event-monitoring

As mentioned in Subsection 1.2.2, continuous monitoring of ETC is inconsistent with the objective of implementing an event-triggered protocol for reducing resource utilization. Approaches seen in the literature to avoid continuous event-monitoring are PETM, self-triggered protocols [36], and use of internal models [37].

In PETM, the ETC is checked at discrete EMIs. Analogous to sample-data control, in most cases, there exists an upper bound on the interval between EMIs. For example, in sample-data control, there exists a maximum sampling interval that results in the spectral radius of the closed-loop system matrix

exceeding one. This leads to instability of the equivalent discretized system according to [38]. The implication of this for PETMs is that the sampling interval must be selected such that when the PETM becomes redundant, reducing the event-triggered protocol to sample-data control, the MAS must still be capable of achieving consensus in some sense. In addition to [38], the authors of [39] and [27] also presented techniques for pre-computing the maximum allowable sampling period (MASP), by utilizing Lyapunov stability theorem, such that the control objective is guaranteed.

In the self-triggered approach, the next sampling instant is predicted at the current sampling instant based on presently available information and model of the system dynamics. Typically, the prediction is made by again using the Lyapunov stability theorem to determine the future time instant at which the condition for some notion of consensus ceases to be met, see [40]. The challenge of this approach is the persistent computation required at each current sampling instant to compute the subsequent future sampling instant.

In the internal model approach, as demonstrated in [41], each agent obtains samples of neighbouring agents' states and propagate those states internally, which is then utilized to distributively check for events. As a similar consequence to the self-triggered approach, this approach consumes excessive computational resources in an already resource limited situation. In addition, when disturbances exist, internal models can become wildly inaccurate.

Of the mentioned approaches, the use of PETM with pre-computed upper bound on sampling interval is more consistent with the intention of reducing resource consumption. It is worth mentioning that in some special cases, the combination of distributed MAS with ASMs and a CTETM with time-based ETC has also demonstrated to not require continuous monitoring of neighbouring agents. This is at the cost of the implications involved with implementing a time-based ETC as mentioned in Subsection 1.2.2.

1.3 Research Gap

To recapitulate Section 1.1, this thesis studies the MAS consensus problem, involving modern agents, and the design of an ETM that is realistic for implementation on digital hardware. Based on our literature survey in Section 1.2, we believe research potential exists in this regard. In the work by [23], the authors facilitated asynchronous broadcasts but did not consider MASs

with RSMs or sensing capabilities. Meanwhile, in [20], the authors considered linear MASs with RSMs and quantization effects but the ETMs used were continuously evaluated, which might not be suitable for digital implementation. Whereas in [19], the authors implemented periodic event-monitoring through the self-triggered approach, which might result in higher computational demand due to sequential computation of EMIs. Lastly, in [42], the authors considered a double integrator MAS under a directed network but the PETM was static and utilized a purely time-based ETC. To the best of our knowledge, we believe that the distributed MAS consensus problem, utilizing undirected graph and RSM sensing, combined with a dynamic PETM - where the EMIs are explicitly pre-computed individually for each agent - remains under-explored and warrants further study.

1.4 Thesis Contribution

Given the research gaps identified in Section 1.3, the specific contributions of this thesis are summarized as follows:

- We construct and establish sufficient conditions for the parameters of the dynamic PETMs[3], designed according to the framework developed in [35], that solve the distributed MAS consensus problem, where agents possess homogeneous linear time-invariant (LTI) dynamics and utilize undirected interaction topology combined with RSM sensing capabilities.

- We derive an expression to explicitly pre-compute the upper bound on event-monitoring interval for the dynamic PETM, individually, for each agent. This is such that asynchronous event-monitoring between agents is supported while guaranteeing consensus of the MAS.

1.5 Thesis Outline

The layout of the remainder of this thesis has been organized into the following chapters. Chapter 2 introduces preliminary concepts that enhance the clarity of our main results in the subsequent chapters. Chapter 3, as a

[3]Although the ETM designed in this thesis is not necessarily periodic, we continue to use the phrase *periodic* ETM for historical reasons (see [35]).

proof of concept, establishes and executes our contributions outlined in Section 1.4 for agents possessing single-integrator dynamics. Chapter 4 extends the work of Chapter 3 to agents with LTI dynamics and for two dynamic PETM constructions, thereby delivering on our contributions listed in Section 1.4. Lastly, Chapter 5 concludes the work within this thesis and offers possible future directions for further exploration. Unless otherwise explicitly defined, all variables used in this thesis are to be considered vectors.

Chapter 2

Preliminaries

In this chapter, we introduce and detail preliminaries regarding graph theory, RSM formulation, dynamic PETM, hybrid system framework, and approaches to show consensus. The preliminaries aid in enhancing the clarity of our main results within the subsequent chapters. We must emphasize that the concepts and work presented in this chapter do not constitute as our contributions; the credit should be given to the referenced authors.

2.1 Algebraic Graph Theory

Introduced in Subsection 1.2.1, the AGT effectively models the information flow between agents within a MAS. According to [15], $\mathcal{G} = (\mathcal{V}(\mathcal{G}), \mathcal{E}(\mathcal{G}))$ denotes a graph with N-nodes where $\mathcal{V}(\mathcal{G}) = \{1, \cdots, N\}$ is the node (agent) set and $\mathcal{E}(\mathcal{G}) \in \{\mathcal{V}(\mathcal{G}) \times \mathcal{V}(\mathcal{G})\}$ is the edge set representing the link between nodes. Node j is called a *neighbour* of node i if the edge $(j, i) \in \mathcal{E}(\mathcal{G})$, that is, information can flow from node j to node i. The graph $\mathcal{G}$ is called *undirected* iff $(j, i) \in \mathcal{E}(\mathcal{G}) \iff (i, j) \in \mathcal{E}(\mathcal{G})$ for all $i, j \in \mathcal{V}(\mathcal{G})$. In addition, the graph $\mathcal{G}$ is *connected* if there exists a path, comprising of a sequence of edges in $\mathcal{E}(\mathcal{G})$, between any two nodes in $\mathcal{V}(\mathcal{G})$.

Graphs are frequently used to model binary relationships between nodes; but, for greater generality, one may also incorporate weightings to represent the strength of the relationship. Adopting the latter, each edge in $\{\mathcal{V}(\mathcal{G}) \times \mathcal{V}(\mathcal{G})\}$ is assigned a weight, a_{ij}, where $a_{ij} > 0$ for $(j, i) \in \mathcal{E}(\mathcal{G})$, else $a_{ij} = 0$ and $a_{ii} = 0$ (assuming no self-loops), $\forall i, j \in \mathcal{V}(\mathcal{G})$. The *adjacency matrix* and *degree matrix* of the $\mathcal{G}$ is denoted, respectively, as $\mathcal{A}(\mathcal{G}) = [a_{ij}]_{N \times N}$ and $\mathcal{D}(\mathcal{G}) = \mathsf{diag}([d_1, .., d_N])$, where $d_i = \sum_{j=1}^{N} a_{ij}$. The graph *Laplacian matrix* is

then defined as $L(\mathcal{G}) = \mathcal{D}(\mathcal{G}) - \mathcal{A}(\mathcal{G})$.

For an undirected and connected graph, some convenient properties exist. These properties are $L(\mathcal{G}) = L(\mathcal{G})^T$ and the eigenvalues of $L(\mathcal{G})$ are such that $0 = \Lambda_1(L(\mathcal{G})) < \Lambda_2(L(\mathcal{G})) \leq ... \leq \Lambda_N(L(\mathcal{G}))$. Additionally, $L(\mathcal{G})$ can be diagonalized such that $L(\mathcal{G}) = M\Lambda(L(\mathcal{G}))M^T$, where $\Lambda(L(\mathcal{G}))$ is a diagonal matrix comprising of the eigenvalues of $L(\mathcal{G})$ and M is the corresponding matrix of eigenvectors of $L(\mathcal{G})$ with $MM^T = I_N$.

It will be seen in the main results that the Lapalcian matrix and these convenient properties facilitate defining of stack vectors as well as establishing upper bounds in consensus errors.

2.2 RSM Formulation

Highlighted in Subsection 1.2.1, information exchange between agents for control can occur through ASMs or RSMs. Figure 2.1 illustratively highlights the difference between the two capabilities. According to [9], typically for a CT controller, the input for each agent in $\mathcal{V}(\mathcal{G})$ which solves the MAS consensus problem takes the form[1]:

$$u_i(t) = -\sum_{j=1}^{N} a_{ij}(x_i(t) - x_j(t)), \tag{2.1}$$

where a_{ij} is associated with the graph and $x_i(t)$ represents the state of agent i. The employment of ASMs or RSMs is not distinguishable within eq (2.1), as they are both equivalent for a CT controller. However, the distinction is pronounced when DT controller (or, sample-data and, by extension, event-triggered protocol) is employed. Illustrating with a sample-data controller with zero-order hold, let s_k^i denote the k-th sampling instant of agent i. Then the input for agent i when utilizing ASM takes the form:

$$u_i(t) = -\sum_{j=1}^{N} a_{ij}(x_i(s_k^i) - x_j(s_{k'}^j)),\ t \in [s_k^i, s_{k+1}^i), \tag{2.2}$$

[1]It is often assumed that there exists a CT controller which solves the consensus problem for the MAS. Since CT controllers exhibit the most active control intervention, the nonexistence of such a controller implies that no other forms of control protocol which sacrifices control performance, e.g. sample-data or event-triggered strategies, is capable of solving the consensus problem.

where $s^j_{k'}$ denotes the latest sampling instant of agent j. Hence, it can be seen in eq (2.2) that the control input for agent i updates both at its own sampling instant and the sampling instant of any of its neighbours. For the same sample-data controller, the control input for agent i when utilizing RSM takes the form:

$$u_i(t) = -\sum_{j=1}^{N} a_{ij}(x_i(s^i_k) - x_j(s^i_k)),\ t \in [s^i_k, s^i_{k+1}). \tag{2.3}$$

In eq (2.3), the control update of agent i occurs only at its own sampling instant as a result of agent i's capability of directly measuring the states of its neighbours. In both eq (2.2) and eq (2.3), the agents' state(s) at event-triggering instant, $x_i(s^i_k)$, can be equivalently represented in terms of the agent's CT state(s) with an error variable. That is, as an example, $e_i(t) = x_i(s^i_k) - x_i(t)$. Such a reformulation facilitates mathematical manipulation and control analysis by treating the error as an input.

It will be seen in the main results that the general form of eq (2.3), followed by reformulation to encompass a measurement error variable, is utilized to model the relative-state sensing capabilities and event-triggered protocols for the MAS.

(a) (b)

Figure 2.1: Illustration of ASM via broadcast of position in (a), and RSM via lidar to obtain distance in (b).

2.3 Hybrid System Framework

Motivated by the intent to unify the CT dynamics of physical agents with the DT updates of digital controllers, as mentioned in Section 1.1, the hybrid system framework introduced in [43] is well-suited for this purpose. Existing references that employed the hybrid system framework for the aforementioned reason include [27], [44], and [21]. Figure 2.2 provides an illustration of the

position trajectory of a bouncing ball modelled in the hybrid system framework, where the ball possesses CT dynamics as it travels in the air and DT dynamics as it impacts the ground (instantaneous switching of direction of travel).

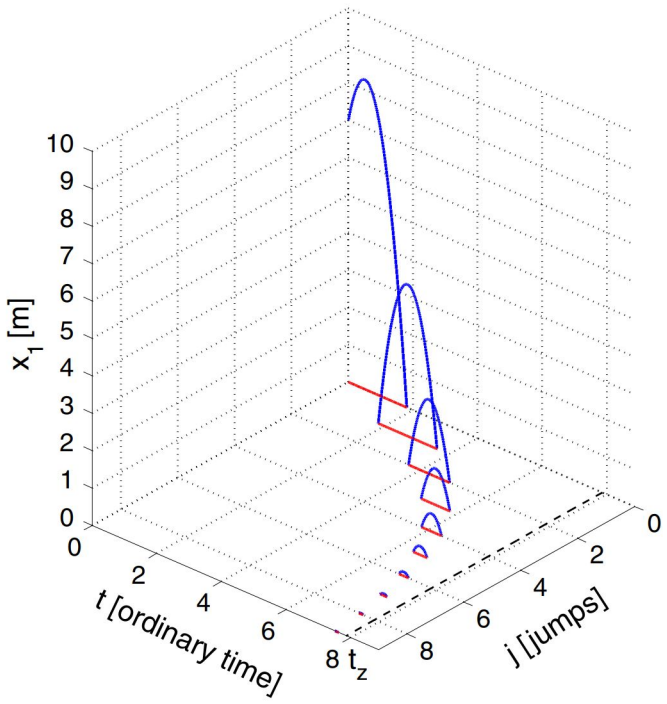

Figure 2.2: Example of a hybrid domain and hybrid arc for a bouncing ball [45].

To establish the hybrid system framework, let $\xi \in \mathbb{R}^n$ denote the hybrid arc, which will formally be defined later in this section. A hybrid system $\mathcal{H} = (C, F, D, G)$ consists of CT dynamics, namely, flows, and DT dynamics, namely, jumps. $\mathcal{H}$ can be expressed mathematically as:

$$\begin{aligned} \dot{\xi} &= F(\xi),\ \xi \in C, \\ \xi^+ &\in G(\xi),\ \xi \in D, \end{aligned} \tag{2.4}$$

where:

- $C \in \mathbb{R}^n$, is the flow set in which the continuous state ξ evolves,
- $F:\ C \to \mathbb{R}^n$, is called the flow map,
- $D \in \mathbb{R}^n$, is the jump set in which the state ξ must belong to, to enable jump,

- $G:\ D \rightrightarrows \mathbb{R}^n$, is a set-valued mapping (indicated by the double arrow) called the jump map.

In eq (2.4), notice that ξ^+ (or ξ after jump) is a difference inclusion rather than an equality. This is to capture different jump maps based on operating modes. To ensure the existence and uniqueness of solutions, the hybrid system of eq (3.10) must satisfy what are called the *hybrid basic assumptions*, which state:

- C and D are closed sets in $\mathbb{R}^n$,
- F is outer semi-continuous, locally bounded on C, and non-empty and convex for each $\xi \in C$,
- G is outer semi-continuous, locally bounded on D, and non-empty for each $\xi \in D$.

Unlike purely CT variables which are parametrized by time, $t \in \mathbb{R}_{\geq 0}$, or purely DT variables which are parametrized by iteration, $j \in \mathbb{N}_{\geq 0}$, hybrid arcs are parametrized by both time and iteration. A compact hybrid time domain of a hybrid arc is a stitching of a sequence of time intervals concatenated with the associated jump sequence. Formally, a compact hybrid time domain, E, is defined as:

$$E = \bigcup_{j=0}^{J-1} ([t_j, t_{j+1}], j) \ \subset \mathbb{R}_{\geq 0} \times \mathbb{N}_{\geq 0}, \tag{2.5}$$

where $0 = t_0 \leq t_1 \leq \cdots \leq t_J \in \mathbb{R}_{\geq 0}$, and $J \in \mathbb{N}_{\geq 0}$. E is a hybrid time domain if $E \cap ([0, T] \times \{0, 1, \cdots, J\})$ is a compact hybrid time domain $\forall (T, J) \in E$. The hybrid time domain for the bouncing ball is illustrated in Figure 2.2 by the red trace. The hybrid arc $\xi:\ \mathsf{dom}\,\xi \to \mathbb{R}^n$ is a locally absolutely continuously differentiable function on the intervals $I^j = \{t : (t, j) \in \mathsf{dom}\,\xi\},\ \forall j \in \mathbb{N}_{\geq 0}$. ξ is a solution to $\mathcal{H}$ if:

- $\xi(0, 0) \in C \cup D$,
- The flow condition is satisfied, where for each $j \in \mathbb{N}_{\geq 0}$, I^j contains a non-empty interior such that:

$$\dot{\xi}(t, j) \in F(\xi(t, j)) \text{ for almost all t} \in I^j, \tag{2.6}$$

$$\xi(t, j) \in C, \text{ for all t} \in I^j, \tag{2.7}$$

- The jump condition is satisfied, where for each $(t, j) \in \mathsf{dom}\,\xi$, $(t, j+1) \in \mathsf{dom}\,\xi$ and such that:

$$\xi(t, j+1) \in G(\xi(t, j)), \tag{2.8}$$

$$\xi(t, j) \in D. \tag{2.9}$$

It will be seen in the main results that the distributed MAS consensus problem with a dynamic PETM is modelled and analysed using the hybrid system framework construction presented within this section. The approaches to show consensus of the MAS modelled in the hybrid system framework will be later described in Section 2.5.

2.4 Dynamic PETM

Described in Subsection 1.2.2, a PETM checks event-conditions at predetermined EMIs. Meanwhile, a dynamic threshold ETC utilizes an auxiliary variable and reduces the likeliness of events by considering the cumulative effects of agents' trajectories. The use of a PETM with a dynamic threshold ETC lends to a dynamic PETM protocol, for which a general design framework was developed in [35]. In the referenced framework, for each agent $i \in \mathcal{V}(\mathcal{G})$, it defines a lower-bound, ε^i, and upper-bound, T^i, on the event-monitoring intervals as:

$$\varepsilon^i \leq s^i_{k+1} - s^i_k \leq T^i,\ \forall k \in \mathbb{N}_{\geq 0}, \tag{2.10}$$

where $k \in \mathbb{N}_{\geq 0}$. Here, ε^i is an arbitrarily small positive constant[2] and T^i denotes the MASP, which is to be determined. Previously mentioned in Subsection 1.2.3, [38] and [39] presented possible techniques to computing the MASP. Let $\{s^i_k\}^\infty_{k=0}$ denote the sequence of predetermined EMIs for agent i, which may be selected differently for each agent, of when neighbour information are sampled and ETCs verified. Additionally, for $l \in \mathbb{N}_{\geq 0}$, let t^i_l and $\{t^i_l\}^\infty_{l=0}$ denote the l-th event-triggering instant and the sequence of all triggering instants of agent i, respectively. Then the PETM, which dictates when the next event is triggered, and thus when control is updated, is governed by:

$$t^i_{l+1} = \inf\{t > t^i_l \mid t \in \{s^i_k\}^\infty_{k=0},\ g^i_s(\cdot) < 0\}. \tag{2.11}$$

[2] ε^i possesses both practical and theoretical implications: 1) practically, ε^i is associated with the maximum sampling frequency of an agent's hardware, and 2) theoretically, ε^i guarantees that Zeno-behaviour is avoided by construction, see article by [27].

It can be seen from eq (2.11) that events can only be triggered at EMIs. That is, $\{t_l^i\}_{l=0}^{\infty} \subset \{s_k^i\}_{k=0}^{\infty}$. In the scenario when the PETM of eq (2.11) becomes redundant, then the protocol simply reduces to sample-data control, in other words, $\{t_l^i\}_{l=0}^{\infty} = \{s_k^i\}_{k=0}^{\infty}$. The inequality $g_s^i(\cdot) < 0$ represents the dynamic ETC to be designed.

Before establishing the auxiliary variable for the dynamic ETC, first let $\varrho_{\bar{N}_i}(t_l^i) \in \mathbb{R}^{nN}$ represent the vector sum of RSMs that are accessible to agent i at the triggering instant t_l^i. In addition, let $e_i^i(t)$ represent some measurement error construction for agent i associated with the implementation of the event-triggered protocol. Now, defining the auxiliary variable of the dynamic ETC, let $\eta_i \in \mathbb{R}_{\geq 0}$ be a non-negative variable whose hybrid dynamics are governed by:

$$\begin{aligned} \dot{\eta}_i(t) &= f_\eta^i(\eta_i(t), \varrho_{\bar{N}_i}(t_l^i)),\ t \in [s_k^i, s_{k+1}^i), \\ \eta_i^+ &= \begin{cases} g_s^i(\eta_i(t), e_i^i(t)),\ t \in \{s_k^i\} \setminus \{t_l^i\}, \\ g_t^i(\eta_i(t), e_i^i(t)),\ t \in \{t_l^i\}, \end{cases} \end{aligned} \tag{2.12}$$

where f_η^i is a continuous function, g_s^i is the jump map at s_k^i when an event is not triggered, and g_t^i is the jump map at s_k^i when an event is triggered. Furthermore, the initial condition, $\eta_i(0)$, is a positive constant design parameter to be selected. From eq (2.12), it can be seen that only local, available, and intermittent information is being utilized in the dynamic ETC, i.e., information $e_i^i(t)$ and $\varrho_{\bar{N}_i}(t)$ are not available to agent i during $t \in (s_k^i, s_{k+1}^i), \forall k \in \mathbb{N}$. As well, the agents do not employ any kind of global information, thus lending to the protocol being distributed. As it is necessary to track the time elapsed since the last EMI to determine the subsequent instant to check for event, a timer variable naturally accompanies the construction of a PETM. The timer variable for each agent is defined as $\tau^i \in \mathbb{R}_{\geq 0}$, and its hybrid dynamic follows:

$$\begin{aligned} \dot{\tau}_i &= 1,\ \forall t \in [s_k^i, s_{k+1}^i), \\ \tau_i^+ &= 0,\ \forall t \in \{s_k^i\}_{k=0}^{\infty}. \end{aligned} \tag{2.13}$$

It will be seen in the main results that T^i is established individually for each agent, and the selection of event-monitoring intervals follows eq (2.10). Furthermore, the construction of the dynamic PETM, to achieve our contributions listed in Section 1.4, is in accordance with eq (2.11) and eq (2.12).

2.5 Approaches to Show Consensus

Equally important as the aforementioned framework, protocols, and approaches, are the mathematical theory and tools to guarantee the convergence of the system states to the control objective, which in our case is consensus. Typically, consensus for MAS employing CTETM is proven in the sense of Lyapunov as demonstrated in [34], [30], and [46]. That is, selecting a Lyapunov function candidate $V(\cdot)$ and taking the consensus error variable $z(t)$, as an argument, such that:

$$V(z) > 0, \tag{2.14}$$

$$\dot{V}(z) \leq -\psi(V(z)), \tag{2.15}$$

where $\psi(\cdot) : \mathbb{R} \to \mathbb{R}_{\geq 0}$ is a positive-definite function of its argument.

In the case where a time-based threshold ETC is utilized, satisfying the conditions for consensus in the sense of Lyapunov may not be immediately apparent due to the time-decaying function. The Barbalat's lemma [47], together with the Comparison lemma can be utilized to show that the time derivative of the Lyapunov function approaches zero at time approaches infinity. This technique was employed in [24] where the authors showed that:

$$\lim_{t\to\infty} \int_0^t \dot{V} dt = \lim_{t\to\infty} V(t) - V(0) \leq \mathsf{constant}, \tag{2.16}$$

implying $\dot{V}(t) \to 0$ as $t \to \infty$ and that z is at least bounded. To prove that consensus occurs, that is, $z(t) \to 0$ as $t \to \infty$, a similar approach to eq (2.16) was employed by the authors on:

$$\lim_{t\to\infty} \int_0^t z(t)^T z(t) dt \leq \mathsf{constant}. \tag{2.17}$$

To prove consensus of the MAS in the hybrid system framework, it is necessary to show that the consensus variable and the measurement error components of the hybrid arc converges to zero both during flows and after jumps. It is worth noting that we do not need the hybrid arc, ξ, to necessarily converge to zero due to the inclusion of auxiliary variables, like the timer variable, which perpetually grow and resets. The Lyapunov stability theorem is once again utilized. For a hybrid arc, ξ, a typical Lyapunov function candidate to the hybrid system is defined as $U(\xi) = V(z) + W(e)$, where V and W

are positive-definite functions of its argument. The conditions for consensus of the MAS, in the sense of Lyapunov, within the hybrid system framework are:

$$V(z) > 0,\ W(e) > 0, \tag{2.18}$$

$$\dot{U}(\xi) \leq -\psi(U(\xi)),\ \forall \xi \in C, \tag{2.19}$$

$$U(\xi^+) - U(\xi) \leq 0,\ \forall \xi \in D. \tag{2.20}$$

It will be seen in the main results that eq (2.18) - eq (2.20) are verified in order to guarantee consensus of the MAS with the implementation of a dynamic PETM.

Chapter 3

Single-integrator MAS

In this chapter, we deliver one of our main results which is establishing and executing the contributions listed in Section 1.4 but for agents possessing homogeneous single-integrator dynamics. This chapter serves as the foundation for our subsequent chapter, which extends the agents' dynamics to LTI systems. The MAS structure that we are investigating is illustrated in Figure 3.1. For the outline of this chapter, we first define our problem formulation by leveraging the preliminaries presented in Chapter 2. Then we present the expression to explicitly pre-compute the MASP, and we introduce our theorem that constructs and establishes the sufficient conditions for the dynamic PETM, together with which consensus is guaranteed. Finally, we demonstrate the effectiveness of our designed protocol with a numerical example and simulation.

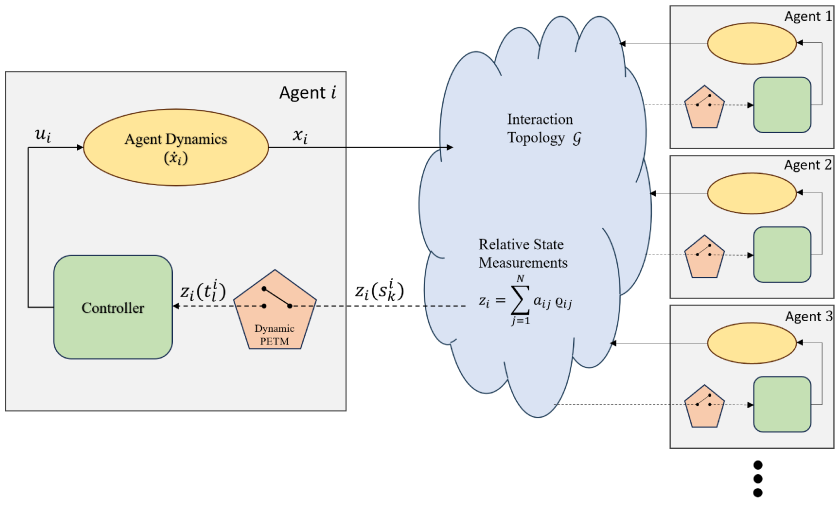

Figure 3.1: Illustration of the MAS structure.

3.1 Problem Formulation

Consider an N-agent ($N \geq 2$) MAS coordinating over an undirected and connected interaction topology defined by $\mathcal{G} = (\mathcal{V}, \mathcal{E})$, as previously introduced in Section 2.1. The dynamics of each agent in the network is homogeneous and follows:

$$\begin{aligned} \dot{x}_i(t) &= u_i(t), \\ x_i^+(t) &= x_i(t), \ \forall i \in \mathcal{V}, \end{aligned} \tag{3.1}$$

where $x_i(t) \in \mathbb{R}^n$ and $u_i(t) \in \mathbb{R}^n$ represents the state[1] and the control input of each agent in the topology, respectively. We denote $x(t) = [x_1^T(t), ..., x_N^T(t)]^T \in \mathbb{R}^{nN}$ as the stacked state vector of the overall MAS.

Since we are interested in solving the consensus problem by employing RSMs, as previously introduced in Section 2.2, and with an event-triggered protocol, the control input for each agent $i \in \mathcal{V}$ is designed as:

$$u_i(t) = -\hat{z}_i(t), \tag{3.2}$$

$$\hat{z}_i(t) = z_i(t_l^i) = \sum_{j=1}^{N} a_{ij} \varrho_{ij}(t_l^i), \ t \in [t_l^i, t_{l+1}^i). \tag{3.3}$$

Here, for every $i, j \in \mathcal{V}$, we define $\varrho_{ij}(t) = x_i(t) - x_j(t)$ as the RSM between agent i and j, and t_l^i is the l-th event-triggering instant of agent i, as previously defined. It can be seen in eq (3.2) that, owing to the distributed event-triggered protocol, agent i's control input is only updated during its sequence of event-triggering instants $\{t_l^i\}_{l=0}^{\infty}$. Between events, the control input is held constant (i.e. zero-order hold) potentially leading to reduced resource consumption and actuator wear (by avoiding high frequency actuation updates).

Next, we define the RSM error between any two agents $i, j \in \mathcal{V}$ (denoted by the subscript on e) as sensed by agent i (denoted by the superscript on e) as:

$$e_{ij}^i(t) = a_{ij}(\varrho_{ij}(t_l^i) - \varrho_{ij}(t)), \ t \in [t_l^i, t_{l+1}^i). \tag{3.4}$$

Similarly, we let $e_i^i(t) = [e_{i1}^{iT}(t), ..., e_{iN}^{iT}(t)]^T \in \mathbb{R}^{nN}$ and $e(t) = [e_1^{1T}, ..., e_N^{NT}]^T \in \mathbb{R}^{nN^2}$ denote the stacked vectors of the RSM errors associated with agent i and the overall MAS, respectively. It is worth noting that, again owing to the distributed protocol and error construction, $e_{ij}^i(t)$ may not be equal to

[1]Please note, we employ the n-dimension state vector for each agent, even in the case for single-integrator agents, in order to allow for broader generalization. This enables us to maintain the same notations in the subsequent chapter with LTI agent dynamics.

$-e^j_{ji}(t)$ due to different event-triggering instants of the agents i and agent j. With eq (3.4), the agents' state dynamics in eq (3.1) and the dynamics of the stacked state vector of the MAS can be, respectively, represented as:

$$\dot{x}_i = -(L_i \otimes I_n)x - \sum_{j=1}^{N} e^i_{ij},\ \forall i \in \mathcal{V}, \tag{3.5}$$

$$\dot{x} = f_x(x, e) = -(L \otimes I_n)x - \tilde{I}e, \tag{3.6}$$

where L_i is the i-th row of the Laplacian matrix, L, and $\tilde{I} = (I_N \otimes \mathbf{1}_N^T) \otimes I_n$. Similarly, the dynamics of both e^i_{ij} and the stacked error vector e are given by:

$$\dot{e}^i_{ij} = a_{ij}\Big(e^i_{ij} + \big((L_i - L_j) \otimes I_n\big)x + \sum_{p\in\mathcal{V}\setminus\{j\}} e^i_{ip} - \sum_{p\in\mathcal{V}} e^j_{jp}\Big), \quad t \in [t^i_l, t^i_{l+1}), \tag{3.7}$$

$$e^{i+}_i = \begin{cases} e^i_i,\ t \in \{s^i_k\} \setminus \{t^i_l\}, \\ h(e^i_i),\ t \in \{t^i_l\}, \end{cases} \tag{3.8}$$

$$\dot{e} = g_e(x, e) = \big(\mathsf{diag}(\{a_{ij}\}_{i,j\in\mathcal{V}}) \otimes I_n\big)\Big[\Big(\big((I_N \otimes \mathbf{1}_N - \mathbf{1}_N \otimes I_N)L\big) \otimes I_n\Big)x + \big((I_N \otimes \mathbf{1}_N\mathbf{1}_N^T - \mathbf{1}_N \otimes I_N \otimes \mathbf{1}_N^T) \otimes I_n\big)e\Big], \tag{3.9}$$

$\forall i, j, \in \mathcal{V}$ and where $h(\cdot)$ is a mapping function for the reset of the RSM error. Attributed by the interaction topology's connectivity, it can be seen in eq (3.4) and eq (3.7) that when $(j, i) \notin \mathcal{E} \rightarrow a_{ij} = 0$, then $e^i_{ij}(t) = \dot{e}^i_{ij}(t) = 0$ as that edge does not contribute to control, i.e., $a_{ij} = 0$.

In terms of implementation, CTETM poses a concern because it implies that CT sensing/monitoring is necessary; this is resource inefficient and, more importantly, digitally unimplementable. For our problem formulation, we choose a dynamic PETM in order to avoid continuous event monitoring and to reduce the likeliness of event occurrence compared to a static PETM, according to [48]. For the formulation of the dynamic PETM, we refer to Section 2.4 of our preliminaries chapter. However, we just denote $\eta(t) = [\eta_1(t), \cdots, \eta_N(t)]^T \in \mathbb{R}^N_{>0}$ and $\dot{\eta}(t) = f_\eta(\eta(t), x(t), e(t)) \in \mathbb{R}^N$ as the stacked auxiliary variable vector and its dynamics for the MAS, respectively, while the stacked timer vector is denoted as $\tau = [\tau_1, ..., \tau_N]^T \in \mathbb{R}^N_{\geq 0}$. The specific construction of eq (2.12) and the design parameter selection for our problem

is later presented in our Theorem 1. Furthermore, it will be demonstrated in Section 3.2 that the magnitude of T^i of each agent is influenced by the individual agent's gain associated with their corresponding RSM errors. Lastly, we assume that when the ETC in eq (2.11) is satisfied, then $e_i^{i^+}(t) = h(e_i^i) = \mathbf{0}_N$, else $e_i^{i^+}(t) = e_i^i(t)$. That is, we do not consider the effects of quantization which can be mapped by the function $h(\cdot)$, according to [27].

We form the hybrid dynamical system by unifying the contributions of eq (2.11), eq (2.12), eq (2.13) for each agent, along with eq (3.6) and eq (3.9). For brevity, we sometimes drop function and variable arguments. Let the hybrid arc (signal) for the MAS be defined as $\xi = (x, e, \tau, \eta) \in \mathbb{X} = \mathbb{R}^{nN} \times \mathbb{R}^{nN^2} \times \mathbb{R}^N_{\geq 0} \times \mathbb{R}^N_{\geq 0}$. According to Section 2.3, then the hybrid system, $\mathcal{H}$, can be expressed as:

$$\begin{aligned} \dot{\xi} &= F(\xi),\ \xi \in C, \\ \xi^+ &\in G(\xi),\ \xi \in D, \end{aligned} \tag{3.10}$$

where the flow set, C, and jump set, D, are domain sets defined as:

$$C = \{\xi \in \mathbb{X} \mid 0 \leq \tau^i \leq T^i,\ \forall i \in \mathcal{V}\}, \tag{3.11}$$

$$\begin{aligned} D = \bigcup_{i=1}^{N} \{\mathbb{R}^{nN} \times \mathbb{R}^{nN^2} \times [0, T^1] \times \cdots \underbrace{[\varepsilon^i, T^i]}_{\substack{\text{timer } \tau_i \text{ of} \\ \text{agent } i \text{ entering jump}}} \cdots \times \\ \cdots [0, T^N] \times \mathbb{R}^N_{\geq 0}\}. \end{aligned} \tag{3.12}$$

It can be seen from eq (3.11) that when all agents flow, then the hybrid signal $\xi \in C$. On the other hand, if any agent in $\mathcal{V}$ experiences a jump, then the hybrid signal ξ must have been in D. $F(\xi)$ and $G(\xi)$ from eq (3.10) are defined as:

$$F(\xi) = [f_x^T, g_e^T, \mathbf{1}_N^T, f_\eta^T]^T, \tag{3.13}$$

$$G(\xi) = \bigcup_{i=1}^{N} G_i(\xi), \tag{3.14}$$

where:

$$G_i(\xi) = \begin{cases} \begin{cases} \{G_i^s\}, & g_s^i > 0 \\ \{G_i^t\}, & g_s^i < 0 \\ \{G_i^s, G_i^t\} & g_s^i = 0 \end{cases} & \tau_i \in [\varepsilon^i, T^i], \\ \emptyset, & \tau_i \notin [\varepsilon^i, T^i]. \end{cases} \tag{3.15}$$

Here, $G_i^s = [x^T, e^T, (\mathcal{I}_i\tau)^T, (\mathcal{I}_i\eta + \bar{g}_s^i)^T]^T$, $G_i^t = [x^T, ((\mathcal{I}_i \otimes I_{nN})e)^T, (\mathcal{I}_i\tau)^T, (\mathcal{I}_i\eta + \bar{g}_t^i)^T]^T$, $\mathcal{I}_i = \mathsf{diag}(\{1, \cdots, 0, \cdots 1\})$ with 0 at the $i-$th place, $\bar{g}_s^i =$

$[0 \cdots g_s^i \cdots 0]^T$, $\bar{g}_t^i = [0 \cdots g_t^i \cdots 0]^T$ and $\emptyset$ is a null set. We note that the hybrid system, eq (3.10), is nominally well-posed, as defined in [49].

With the MAS formulated as a hybrid system, the objectives for the remainder of this chapter is to: 1) construct the dynamic PETM in accordance with eq (2.12) and establish sufficient conditions for the parameter selection, and 2) obtain the T^i for each agent in $\mathcal{V}$ such that the consensus problem is solved for the MAS in eq (3.1).

3.2 Dynamic PETM Construction

In this section, we employ the Lyapunov stability theorem to compute the event-monitoring intervals governed by eq (2.10) and construct the dynamic PETM governed by eq (2.12). To that effect, we first introduce Assumptions 1 and 2 and Lemma 1, as a *general construction*, which we employ in the proof of our theorem to guarantee consensus of the MAS in eq (3.1).

Assumption 1. For the hybrid system defined in eq (3.10), there exists, $\forall i, j \in \mathcal{V}$:

- a continuous functions $W_{ij}^i(e_{ij}^i) : \mathbb{R}^n \to \mathbb{R}_{\geq 0}$,
- $\underline{\alpha}_{W_{ij}^i}(\cdot)$, $\overline{\alpha}_{W_{ij}^i}(\cdot) \in \mathcal{K}_\infty$,
- scalar functions $H_{ij}(x) : \mathbb{R}^{nN} \to \mathbb{R}_{\geq 0}$ and $J_{ij}(e_i^i, e_j^j) : \mathbb{R}^{2nN} \to \mathbb{R}_{\geq 0}$,
- and a non-negative constant, C_{ij},

such that:

$$\underline{\alpha}_{W_{ij}^i}(\|e_{ij}^i\|) \leq W_{ij}^i(e_{ij}^i) \leq \overline{\alpha}_{W_{ij}^i}(\|e_{ij}^i\|), \tag{3.16}$$

$$\langle \nabla W_{ij}^i(e_{ij}^i),\ \dot{e}_{ij}^i \rangle \leq C_{ij} W_{ij}^i(e_{ij}^i) + H_{ij}(x) + J_{ij}(e_i^i, e_j^j). \tag{3.17}$$

The purpose of Assumption 1 (and eq (3.17)) is to upper-bound the error growth by a sum of non-negative functions.

Assumption 2. Suppose Assumption 1 holds. Assume that for the hybrid system in eq (3.10) there exists:

- a continuous functions $V(x) : \mathbb{R}^{nN} \to \mathbb{R}_{\geq 0}$,
- positive-definite functions $\bar{V}_i^1(\cdot), \bar{V}_i^2(\cdot) : \mathbb{R}_{\geq 0} \to \mathbb{R}_{\geq 0}$,
- class $\mathcal{K}_\infty$-functions $\underline{\alpha}_V(\cdot)$, $\overline{\alpha}_V(\cdot)$,

- state transformation $\Theta(x) : \mathbb{R}^{nN} \to \mathbb{R}^{nN}$,
- functions $z_i(x), \hat{z}_i(x) : \mathbb{R}^{nN} \to \mathbb{R}^n, \forall i \in \mathcal{V}$,
- positive scalars σ, γ_i, $\epsilon_{i,1}$, $\epsilon_{i,2}$, β_i,

such that, $\gamma_i^2 > \epsilon_{i,2}$, and:

$$\underline{\alpha}_V(\|\Theta(x)\|) \leq V(x) \leq \overline{\alpha}_V(\|\Theta(x)\|), \tag{3.18}$$

$$\begin{aligned}\langle \nabla V(x), \dot{x} \rangle \leq & -\sum_{i=1}^{N} \epsilon_{i,1} \bar{V}_i^1(\|z_i\|) - \sum_{i,j=1}^{N} \epsilon_{i,2} (W_{ij}^i)^2 \\ & + \sum_{i,j=1}^{N} \gamma_i^2 (W_{ij}^i)^2 - \sum_{i=1}^{N} \beta_i \bar{V}_i^2(\|\hat{z}_i\|) \\ & - \sigma \sum_{i,j=1}^{N} H_{ij}^2(x) - \sigma \sum_{i,j=1}^{N} J_{ij}^2(e_i^i, e_j^j). \end{aligned} \tag{3.19}$$

Later we will show in the proof of Theorem 1, that with a specific choice of $V(x)$ and with appropriate selection of design parameters, that Assumption 2 is satisfied. Specifically for eq (3.19), this is done by beginning with input-to-state stability (ISS) assumptions and selectively absorbing the effects of the last three terms into the first three terms on the right-hand side of the equation.

Remark 1. As our control objective, in this work, is consensus rather than stabilization, the agent states $x_i(t)$ may not necessarily converge to the origin. To facilitate this, we define $\Theta(x) = 0$ in Assumption 2 as a representation of our consensus stabilization set. For a given problem, the choice of transformation $\Theta(x)$ may not be unique. For instance, for the consensus problems over connected undirected networks, we can have $\Theta(x) = (L \otimes I_n)x$, $\Theta(x) = (\sqrt{L} \otimes I_n)x$ or $\Theta(x) = \big((I_N - \frac{1}{N}\mathbf{1}\mathbf{1}^T) \otimes I_n\big)x$. Generally, $z_i(x)$, which will be formally defined later, can be thought of as a function that maps the agents' states to a consensus error state, and $\|z_i(x)\|$ can be interpreted as some measure of distance of x from the stability set $\Theta(x) = 0$.

To derive an explicit expression to compute the MASP, T^i, we slightly modify the framework developed in [39].

Lemma 1. For the gain, $\theta_i(t) \in \mathbb{R}_{\geq 0}$, let its dynamics be modelled by the following differential equation:

$$\dot{\theta}_i(t) = -2\gamma_i\theta_i^2(t) - 2C_i\theta_i(t) - \frac{1}{\sigma}\gamma_i, \ \forall i \in \mathcal{V}, \tag{3.20}$$

where $C_i = \max_{j\in\mathcal{V}}\{C_{ij}\} > 0$ and with the initial condition $\theta_i(0) = \frac{1}{\lambda_i}$, for some choice of $\lambda_i \in (0,1)$. Then, $\theta_i(t)$ monotonously decreases and is such that, for some T^i, $\theta_i(T^i) = \lambda_i$. In order for $\theta_i(t)$ to be non-negative as time progresses given eq (3.20), the reset of $\theta_i(t)$ at each $\{s_k^i\}_{k=0}^{\infty}$ follows $\theta_i(\tau_i^+) = \theta_i(0)$ for $\tau_i \leq T^i$. Solving eq (3.20) and isolating for T^i for the given terminal conditions, derivations omitted as solving the differential equation follows standard procedures, yields the explicit expression:

$$T^i = \begin{cases} \left| \frac{1}{C_i r} atan\left[- \frac{\frac{-2\gamma_i\lambda_i + C_i}{C_i r} - \rho_1}{\frac{-2\gamma_i\lambda_i + C_i}{C_i r}\rho_1 + 1} \right] \right|, & \frac{2}{\sigma}\gamma_i^2 > C_i^2, \\ \left| \frac{2\gamma_i\lambda_i + C_i + \rho_2}{\rho_2(C_i - 2\gamma_i\lambda_i)} \right|, & \frac{2}{\sigma}\gamma_i^2 = C_i^2, \\ \left| - \frac{1}{2C_i r} ln\left[\frac{1 - \frac{-2\gamma_i\lambda_i + C_i}{C_i r}}{\rho_3(\frac{-2\gamma_i\lambda_i + C_i}{C_i r} + 1)} \right] \right|, & \frac{2}{\sigma}\gamma_i^2 < C_i^2, \end{cases} \tag{3.21}$$

for $i \in \mathcal{V}$ and where $r = \sqrt{\left|\frac{2}{\sigma}(\frac{\gamma_i^2}{C_i^2}) - 1\right|}$, $\rho_1 = \frac{\frac{-2\gamma_i}{\lambda_i} + C_i}{C_i r}$, $\rho_2 = -\frac{2\gamma_i}{\lambda_i} + C_i$, $\rho_3 = (1 - \frac{-2\gamma_i\lambda_i^{-1} + C_i}{C_i r})(\frac{-2\gamma_i\lambda_i^{-1} + C_i}{C_i r} + 1)^{-1}$. The magnitude is taken in eq (3.21) due to the fact that we want the positive argument for the MASP.

Remark 2. In the article [39], the range for λ_i is based on the assumption that the measure of error, namely, W_i^i, decreases during jumps in accordance with:

$$W_i^i(e_i^{i^+}) \leq \lambda_i W_i^i(e_i^i), \ \forall t \in \{t_l^i\}. \tag{3.22}$$

From eq (3.15), since $e_i^{i^+} = 0 \rightarrow W_i^i(e_i^{i^+}) = 0$ at every event-triggering instant; therefore, eq (3.22) holds true for any choice of $\lambda_i \in (0,1)$.

With Assumptions 1 and 2 and Lemma 1 introduced, we now present our theorem on the construction and sufficient conditions for the design parameters of the dynamic PETM such that consensus of the MAS, eq (3.1), is achieved.

Theorem 1. For the hybrid system in eq (3.10), consider $V(x) = \frac{1}{2}x^T(L\otimes I_n)x$ and $W_{ij}^i(e_{ij}^i) = \|e_{ij}^i\|, \ \forall i,j \in \mathcal{V}$. If the functions (f_η^i, g_s^i, g_t^i) of the dynamic

PETM described by eq (2.12) are constructed as follows:

$$\begin{aligned} f_\eta^i &= -\alpha_i \eta_i + \beta_i (\hat{z}_i^T \hat{z}_i), \\ g_s^i &= \eta_i + \sigma \sum_{j=1}^{N} \gamma_i (\lambda_i - \frac{1}{\lambda_i} - \frac{\epsilon_{i,2}}{\gamma_i})(W_{ij}^i)^2, \\ g_t^i &= \eta_i + \sigma \sum_{j=1}^{N} \gamma_i (\lambda_i - \frac{\epsilon_{i,2}}{\gamma_i})(W_{ij}^i)^2, \end{aligned} \tag{3.23}$$

where $z_i(x(t)) = (L_i \otimes I_n)x(t)$, $\hat{z}_i = z_i(x(t_l^i))$, and the design parameters $\alpha_i > 0$, $\beta_i \geq 0$, $\sigma > 0$, $\sigma_1 > 0$, and $\epsilon_i > 0$ are such that:

$$Q_i = (1 - \tfrac{1}{2}\sigma_1 - 4\sigma a_{max}^2 N - \epsilon_i) \geq 0,$$

$$\epsilon_{i,2} = (\epsilon_i - 2N\beta_i) > 0.$$

And with T^i computed through Lemma 1 using:

$$C_{ij} = a_{ij},$$

$$\gamma_i^2 = (\tfrac{1}{2\sigma_1} N + 4\sigma a_{max}^2 N^2 + \epsilon_i),$$

$\forall i \in \mathcal{V}$, where $a_{max} = \max_{i,j \in \mathcal{V}}\{a_{ij}\}$, then the closed-loop system is asymptotically stable with respect to $\{x \in \mathbb{R}^{nN} | (M\sqrt{\Lambda(L)}M^T \otimes I_n)x = 0\}$ (stabilizing set for consensus of the MAS).

Remark 3. For clarity, $\sum_{i=1}^{N} \beta_i \bar{V}_i^2(\|\hat{z}_i\|)$ in eq (3.19) represents the contribution from the $\beta_i(\hat{z}_i^T \hat{z}_i)$ component of the dynamic PETMs in eq (3.23). This contribution has the effect of reducing the likeliness of event occurrence by restraining the rate of decay of η_i at the cost of potentially slower rate of consensus.

Remark 4. It is worth mentioning that Theorem 1 only guarantees consensus of the MAS. The performance of the dynamic PETM, in terms of the event frequency, requires tuning of the parameters (which optimal parameter selection is a separate objective). However, as previously mentioned in Section 2.4, in the worst case, the dynamic PETM simply becomes redundant and reduces the event-triggered protocol to sample-data control, thus providing a safety net for avoiding Zeno-behaviour.

Proof. First, we will show that with the specific form of W_{ij}^i, $V(x)$, and conditions on the dynamic PETM design parameters presented under Theorem

1 that the Assumptions 1 and 2 are satisfied. Subsequently, we will show that consensus of the MAS is achieved using the hybrid system Lyapunov function:

$$U(\xi) = V(x) + \sigma \sum_{i,j=1}^{N} \gamma_i \theta_i(\tau_i)(W_{ij}^i(e_{ij}^i))^2 + \sum_{i=1}^{N} \eta_i(t). \tag{3.24}$$

Checking Assumption 1. It is easy to see that for $W_{ij}^i = \|e_{ij}^i\|$, W_{ij}^i can be lower and upper bounded by $\mathcal{K}_\infty$ functions via scalar constants. To upper bound the error growth rate, we employ the dynamics of $e_{ij}^i(t)$, eq (3.7), then:

$$\langle \nabla W_{ij}^i(e_{ij}^i),\ \dot{e}_{ij}^i \rangle = \frac{\langle e_{ij}^i, \dot{e}_{ij}^i \rangle}{\|e_{ij}^i\|} \leq \|\dot{e}_{ij}^i\|, \tag{3.25}$$

$$\leq \|a_{ij}\Big(e_{ij}^i(t) + ((L_i - L_j) \otimes I_n)x(t) \tag{3.26}$$

$$+ \sum_{p \in \mathcal{V}\setminus\{j\}} e_{ip}^i(t) - \sum_{p \in \mathcal{V}} e_{jp}^j(t)\Big)\|,$$

which, by employing series of norm inequalities, leads to:

$$\begin{aligned} \langle \nabla W_{ij}^i(e_{ij}^i),\ \dot{e}_{ij}^i \rangle \leq & \underbrace{a_{ij} W_{ij}^i}_{C_{ij} W_{ij}^i} + \underbrace{a_{ij}\|((L_i - L_j) \otimes I_n)x\|}_{H_{ij}} \\ & \underbrace{+ a_{ij} \sum_{p=1\setminus\{j\}}^{N} W_{ip}^i + a_{ij} \sum_{p=1}^{N} W_{jp}^j}_{J_{ij}}. \end{aligned} \tag{3.27}$$

With the above bound on the error growth rate, given by eq (3.27), Assumption 1 is satisfied. Next we check Assumption 2.

Checking Assumption 2. Diagonalizing $L = M\Lambda(L)M^T$ and taking the new stabilizing set as $\Theta(x) = (M\sqrt{\Lambda(L)}M^T \otimes I_n)x$, we can then express $V(x) = \frac{1}{2}\|\Theta(x)\|^2$. Since L is the Laplacian for a graph that is undirected and connected, then $\Lambda_1(L) = 0$; thus, there exists an $x \neq 0$ such that $\Theta(x) = 0$. It is then clear to see that $V(x)$ can be lower and upper bounded by $\underline{\alpha}_V(\|\Theta(x)\|)$, $\overline{\alpha}_V(\|\Theta(x)\|)$ through scalar constants. Next, taking $z(t) = (L \otimes I_n)x(t)$ as the consensus variable, then:

$$\begin{aligned} \langle \nabla V(x), \dot{x} \rangle &= x^T(L \otimes I_n)\dot{x}, \\ &= x^T(L \otimes I_n)(-(L \otimes I_n)x - \tilde{I}e), \\ &\leq -z^T z + \frac{1}{2}\sigma_1 z^T z + \frac{1}{2\sigma_1}(\tilde{I}e)^T(\tilde{I}e), \\ &\leq -(1 - \frac{1}{2}\sigma_1)\sum_{i=1}^{N} z_i^T z_i + \frac{1}{2\sigma_1} N \sum_{i,j=1}^{N} (W_{ij}^i)^2. \end{aligned} \tag{3.28}$$

We then add and subtract the terms: $\sigma \sum_{i,j=1}^{N} H_{ij}^2$, $\sigma \sum_{i,j=1}^{N} J_{ij}^2$, $\sum_{i=1}^{N} \epsilon_i z_i^T z_i$ and $\sum_{i,j=1}^{N} \epsilon_i (W_{ij}^i)^2$ to eq (3.28). Applying Young's inequality on $\sigma \sum_{i,j=1}^{N} H_{ij}^2$, $\sigma \sum_{i,j=1}^{N} J_{ij}^2$ allows us to obtain the upper bounds:

$$\sigma \sum_{i,j=1}^{N} H_{ij}^2 \leq 4\sigma a_{max}^2 N \sum_{i=1}^{N} z_i^T z_i, \tag{3.29}$$

$$\sigma \sum_{i,j=1}^{N} J_{ij}^2 \leq 4\sigma a_{max}^2 N^2 \sum_{i,j=1}^{N} (W_{ij}^i)^2. \tag{3.30}$$

Incorporating eq (3.29) and eq (3.30) into eq (3.28) then gives:

$$\begin{aligned} \langle \nabla V(x), \dot{x} \rangle \leq & - \sum_{i=1}^{N} \epsilon_i z_i^T z_i - \sum_{i,j=1}^{N} \epsilon_i (W_{ij}^i)^2 \\ & - \sigma \sum_{i=1}^{N} \underbrace{(1 - \frac{1}{2}\sigma_1 - 4\sigma a_{max}^2 N - \epsilon_i)}_{Q_i} z_i^T z_i \\ & + \sum_{i,j=1}^{N} \underbrace{(\frac{1}{2\sigma_1} N + 4\sigma a_{max}^2 N^2 + \epsilon_i)}_{\gamma_i^2} (W_{ij}^i)^2 \\ & - \sigma \sum_{i,j=1}^{N} H_{ij}^2 - \sigma \sum_{i,j=1}^{N} J_{ij}^2. \end{aligned} \tag{3.31}$$

Finally, we add and subtract $\sum_{i=1}^{N} \beta_i \hat{z}_i^T \hat{z}_i$ to eq (3.31) where:

$$\sum_{i=1}^{N} \beta_i \hat{z}_i^T \hat{z}_i \leq \; 2N \sum_{i,j=1}^{N} \beta_i (W_{ij}^i)^2 + 2 \sum_{i=1}^{N} \beta_i z_i^T z_i. \tag{3.32}$$

Then, by selecting parameters in accordance with Theorem 1 - that is, $Q_i \geq$ and $\epsilon_{i,2} = (\epsilon_i - 2N\beta_i) > 0$ (which $\epsilon_{i,1} \geq \epsilon_{i,2}$), $\forall i \in \mathcal{V}$ - the upper bound of $\dot{V}$ becomes:

$$\begin{aligned} \langle \nabla V(x), \dot{x} \rangle \leq & - \sum_{i=1}^{N} \underbrace{(\epsilon_i - 2\beta_i)}_{\epsilon_{i,1}} \underbrace{z_i^T z_i}_{\bar{V}_i^1(\cdot)} \\ & - \sum_{i,j=1}^{N} \underbrace{(\epsilon_i - 2N\beta_i)}_{\epsilon_{i,2}} (W_{ij}^i)^2 + \sum_{i,j=1}^{N} \gamma_i^2 (W_{ij}^i)^2 \\ & - \sum_{i=1}^{N} \beta_i \underbrace{\hat{z}_i^T \hat{z}_i}_{\bar{V}_i^2(\cdot)} - \sigma \sum_{i,j=1}^{N} H_{ij}^2 - \sigma \sum_{i,j=1}^{N} J_{ij}^2, \end{aligned} \tag{3.33}$$

with which Assumption 2 is satisfied. Next we will prove that consensus for the MAS is guaranteed. For the hybrid system defined in eq (3.10) and the Lyapunov function as defined in eq (3.24), we need to show that $U(\xi)$ monotonically decreases over both the flow domain, C, and jump domain, D.

Flow domain. During the flow domain, the time derivative of $U(\xi)$ takes the form:

$$\dot{U} = \dot{V} + \sigma \sum_{i,j=1}^{N} \gamma_i \dot{\theta}_i (W_{ij}^i)^2 + 2\sigma \sum_{i,j=1}^{N} \gamma_i \theta_i W_{ij}^i \dot{W}_{ij}^i + \sum_{i=1}^{N} \dot{\eta}_i. \tag{3.34}$$

Substituting for the associated time derivatives on the right hand side of eq (3.34) with eq (3.20), eq (3.23), eq (3.27), and eq (3.33) yields:

$$\begin{aligned}
\dot{U} \leq & -\sum_{i=1}^{N} \epsilon_{i,1} z_i^T z_i - \sum_{i,j=1}^{N} \epsilon_{i,2} (W_{ij}^i)^2 + \sum_{i,j=1}^{N} \gamma_i^2 (W_{ij}^i)^2 \\
& - \sum_{i=1}^{N} \beta_i \hat{z}_i^T \hat{z}_i - \sigma \sum_{i,j=1}^{N} H_{ij}^2 - \sigma \sum_{i,j=1}^{N} J_{ij}^2 \\
& + \sigma \sum_{i,j=1}^{N} \gamma_i (-2\gamma_i \theta_i^2 - 2C_i \theta_i - \frac{1}{\sigma} \gamma_i)(W_{ij}^i)^2 \\
& + 2\sigma \sum_{i,j=1}^{N} \gamma_i \theta_i W_{ij}^i (C_{ij} W_{ij}^i + H_{ij} + J_{ij}) \\
& + \sum_{i=1}^{N} (-\alpha_i \eta_i + \beta_i \hat{z}_i^T \hat{z}_i).
\end{aligned} \tag{3.35}$$

Again, employing Young's inequality on the cross terms, we can obtain an upper bound represented by:

$$\begin{aligned}
& 2\sigma \sum_{i,j=1}^{N} \gamma_i \theta_i W_{ij}^i (C_{ij} W_{ij}^i + H_{ij} + J_{ij}) \\
& \qquad \leq 2\sigma \sum_{i,j=1}^{N} \gamma_i \theta_i C_i (W_{ij}^i)^2 + 2\sigma \sum_{i,j=1}^{N} (\gamma_i \theta_i W_{ij}^i)^2 \\
& \qquad\qquad + \sigma \sum_{i,j=1}^{N} H_{ij}^2 + \sigma \sum_{i,j=1}^{N} J_{ij}^2.
\end{aligned} \tag{3.36}$$

Incorporating eq (3.36) into eq (3.34) and cancelling like terms, we can show that:

$$\dot{U} \leq -\sum_{i=1}^{N} \epsilon_{i,1} z_i^T z_i - \sum_{i,j=1}^{N} \epsilon_{i,2} (W_{ij}^i)^2 - \sum_{i=1}^{N} \alpha_i \eta_i. \tag{3.37}$$

Since from Theorem 1 $\epsilon_{i,2}$ and $\alpha_i > 0$, as a result, we can obtain:

$$\dot{U}(\xi) \leq -\psi(U(\xi)),\ \forall \xi \in C, \tag{3.38}$$

where $\psi(\cdot) : \mathbb{R} \to \mathbb{R}_{\geq 0}$ is a positive-definite function. Hence, it is shown that $U(\xi)$ monotonically decreases over the flow domain, C.

Jump domain. To show that $U(\xi)$ monotonically decreases over the jump domain, D, we need to show that the Lyapunov function candidate decreases after each jump, i.e., $U(\xi^+) - U(\xi) < 0$. To this end, according to [35], we define the following sets:

$$\Gamma = \{i \in \mathcal{V} \mid t \in \{s_k^i\}_{k=0}^{\infty}, g_s^i < 0\}, \tag{3.39}$$

$$\Psi = \{i \in \mathcal{V} \mid t \in \{s_k^i\}_{k=0}^{\infty}, g_s^i > 0\}, \tag{3.40}$$

$$\Phi = \{\Phi_s, \Phi_t\} = \{i \in \mathcal{V} \mid t \in \{s_k^i\}_{k=0}^{\infty}, g_s^i = 0\}, \tag{3.41}$$

$$\Omega = \{i \in \mathcal{V} \mid t \notin \{s_k^i\}_{k=0}^{\infty}\}, \tag{3.42}$$

where $\Gamma \cup \Psi \cup \Phi \cup \Omega = \mathcal{V}$, and Φ_s and Φ_t are subset of Φ whose agents' jump map are G_i^s and G_i^t, respectively. In other words, we are partitioning the set of agents in the network into set of agents that triggered an event, sampled but did not trigger an event, and are not participating in jump (or simply still flowing). Then:

$$\begin{aligned} U(\xi^+) = V(x^+) &+ \sigma \sum_{i \in \Gamma \cup \Phi_t} \sum_{j=1}^{N} \gamma_i \theta_i^+ (W_{ij}^{i^+})^2 + \sum_{i \in \Gamma \cup \Phi_t} \eta_i^+ \\ &+ \sigma \sum_{i \in \Psi \cup \Phi_s} \sum_{j=1}^{N} \gamma_i \theta_i^+ (W_{ij}^{i^+})^2 + \sum_{i \in \Psi \cup \Phi_s} \eta_i^+ \\ &+ \sigma \sum_{i \in \Omega} \sum_{j=1}^{N} \gamma_i \theta_i^+ (W_{ij}^{i^+})^2 + \sum_{i \in \Omega} \eta_i^+, \end{aligned} \tag{3.43}$$

where employing the jump maps established in eq (3.15) and applying the fact that for $\tau_i \leq T^i \to \theta_i(\tau_i) \geq \theta_i(T^i) = \lambda_i$ (or $-\theta_i(\tau_i) \leq -\lambda_i$), and $x^+ = x$ yields:

$$\begin{aligned} \sigma \sum_{i \in \Gamma \cup \Phi_t} \sum_{j=1}^{N} \gamma_i \theta_i^+ (W_{ij}^{i^+})^2 + \sum_{i \in \Gamma \cup \Phi_t} \eta_i^+ = \\ \sum_{i \in \Gamma \cup \Phi_t} (\eta_i + \sigma \sum_{j=1}^{N} \gamma_i (\lambda_i - \frac{\epsilon_{i,2}}{\gamma_i}) (W_{ij}^i)^2), \end{aligned} \tag{3.44}$$

and:

$$\sigma \sum_{i\in\Psi\cup\Phi_s}\sum_{j=1}^{N}\gamma_i\theta_i^+(W_{ij}^{i^+})^2+\sum_{i\in\Psi\cup\Phi_s}\eta_i^+=\sigma\sum_{i\in\Psi\cup\Phi_s}\sum_{j=1}^{N}\gamma_i(\frac{1}{\lambda_i})(W_{ij}^i)^2 + \sum_{i\in\Psi\cup\Phi_s}(\eta_i+\sigma\sum_{j=1}^{N}\gamma_i(\lambda_i-\frac{1}{\lambda_i}-\frac{\epsilon_{i,2}}{\gamma_i})(W_{ij}^i)^2), \quad (3.45)$$

and:

$$\sigma\sum_{i\in\Omega}\sum_{j=1}^{N}\gamma_i\theta_i^+(W_{ij}^{i^+})^2 \;+\; \sum_{i\in\Omega}\eta_i^+ \;\;=\;\; \sigma\sum_{i\in\Omega}\sum_{j=1}^{N}\gamma_i\theta_i(W_{ij}^i)^2 \;+\; \sum_{i\in\Omega}\eta_i. \quad (3.46)$$

Performing the same set partition on $U(\xi)$, we obtain:

$$U(\xi^+)-U(\xi)\leq-\sigma\sum_{i\in\Gamma\cup\Phi_t}\sum_{j=1}^{N}\epsilon_{i,2}(W_{ij}^i)^2-\sigma\sum_{i\in\Theta\cup\Phi_s}\sum_{j=1}^{N}\epsilon_{i,2}(W_{ij}^i)^2. \quad (3.47)$$

As $\sigma>0$ and $\epsilon_{i,2}>0$, from Theorem 1; hence:

$$U(\xi^+)-U(\xi)\leq 0, \quad (3.48)$$

which shows that $U(\xi)$ monotonically decreases after each jump.

With eq (3.38) and eq (3.48), the proof is completed and asymptotic consensus of the MAS, eq (3.1), with the control protocol, eq (3.2), and dynamic PETM, in accordance with Theorem 1, is guaranteed. Next, we verify the main results of this section as well as the performance of the dynamic PETM with a numerical example.

3.3 Numerical Example and Simulation

In this section, we consider a numerical example involving a 4-agent MAS coordinating under an undirected and connected $\mathcal{G}=(\mathcal{V},\mathcal{E})$ illustrated by Figure 3.2. The agent's dynamics and control input are constructed following eq (3.1) and eq (3.2), respectively.

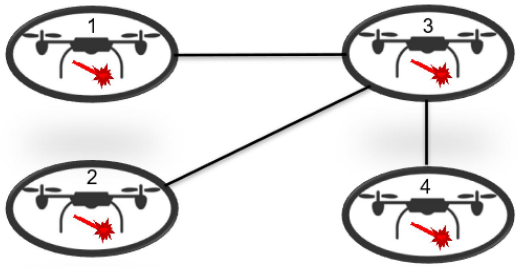

Figure 3.2: MAS interaction topology.

The Laplacian matrix representing $\mathcal{G}$ (considering binary relationship for simplicity) is given by:

$$L = \underbrace{\begin{bmatrix} 1 & 0 & 0 & 0 \\ 0 & 1 & 0 & 0 \\ 0 & 0 & 3 & 0 \\ 0 & 0 & 0 & 1 \end{bmatrix}}_{Degree\ Matrix} - \underbrace{\begin{bmatrix} 0 & 0 & 1 & 0 \\ 0 & 0 & 1 & 0 \\ 1 & 1 & 0 & 1 \\ 0 & 0 & 1 & 0 \end{bmatrix}}_{Adjacency\ Matrix} = \begin{bmatrix} 1 & 0 & -1 & 0 \\ 0 & 1 & -1 & 0 \\ -1 & -1 & 3 & -1 \\ 0 & 0 & -1 & 1 \end{bmatrix}. \tag{3.49}$$

For this example, we select the parameters as follows:

$$\begin{aligned} \sigma_1 &= 1, \\ \sigma &= \frac{1}{16N}, \\ [\epsilon_1, \epsilon_2, \epsilon_3, \epsilon_4] &= [0.05, 0.1, 0.15, 0.2], \\ \alpha_i &= 1,\ \forall i \in \mathcal{V}, \\ [\beta_1, \beta_2, \beta_3, \beta_4] &= [0.0031, 0.0063, 0.0094, 0.0125], \\ \lambda_i &= 0.5,\ \forall i \in \mathcal{V}. \end{aligned}$$

According to Theorem 1, we obtain:

$$\begin{aligned} [Q_1, Q_2, Q_3, Q_4] &= [0.2, 0.15, 0.1, 0.05], \\ C_i &= 1,\ \forall i \in \mathcal{V}, \\ [\gamma_1, \gamma_2, \gamma_3, \gamma_4] &= [1.7464, 1.7607, 1.7748, 1.7889], \\ [\epsilon_{1,1}, \epsilon_{2,1}, \epsilon_{3,1}, \epsilon_{4,1}] &= [0.0438, 0.0875, 0.1313, 0.175], \\ [\epsilon_{1,2}, \epsilon_{2,2}, \epsilon_{3,2}, \epsilon_{4,2}] &= [0.025, 0.05, 0.075, 0.1]. \end{aligned}$$

It can be seen that with our selection of design parameters, $Q_i \geq 0,\ \epsilon_{i,1} > 0$, and $\epsilon_{i,2} > 0,\ \forall i \in \mathcal{V}$. T^is are then explicitly and individually pre-computed

using eq (3.21) for each agent, which we obtain:

$$[T^1, T^2, T^3, T^4] = [0.0130, 0.0129, 0.0128, 0.0127]. \tag{3.50}$$

Hence, if the event-monitoring intervals for each agent is less than T^i for all time, then consensus of the MAS is guaranteed through the proof of Theorem 1.

Remark 5. It is worth noting that the computed T^i in eq (3.50) for each agent are very similar. This is attributed by the fact that λ_i was selected identically the same across all agents. For contrasting λ_i between agents, then there would be greater distinction between the computed T^i. As mentioned in Remark 2, different λ_i may arise by designer selection or dictated by eq (3.22). In the latter, such a scenario could occur if some agents employed quantizers, thus, narrowing the allowable range for λ_i for that agent. Although our results do not consider the effects of quantization, being able to compute the MASP individually for each agent could lay the foundation for scenarios where some agents of the MAS employ quantizers or even non-uniform quantizers.

For the simulation, following eq (2.10), we select the asynchronous periodic[2] event-monitoring intervals for the agents as:

$$[(s^i_{k+1} - s^i_k)]_{\forall i \in \mathcal{V}} = [0.01, 0.0075, 0.012, 0.005]. \tag{3.51}$$

Additionally, we simulate a CTETM, designed in [19], to compare with our results for the same MAS. Figure 3.3 presents the state trajectories of the agents, for both the PETM and CTETM. Based on Figure 3.4, consensus of the MAS with both event-triggered protocols can be observed. Then, Table 3.1 summarizes the event frequencies for both Theorem 1's PETM and the CTETM. Furthermore, Figure 3.5 provides some statistical data with respect to the inter-event times for our dynamic PETM and Figure 3.6 plots the trajectories of the auxiliary variables. Lastly, for the simulation, an integration time step of 1×10^{-4} seconds was used.

[2]An asynchronous aperiodic event-monitoring interval can be utilized for each agent provided eq (2.10) is always satisfied.

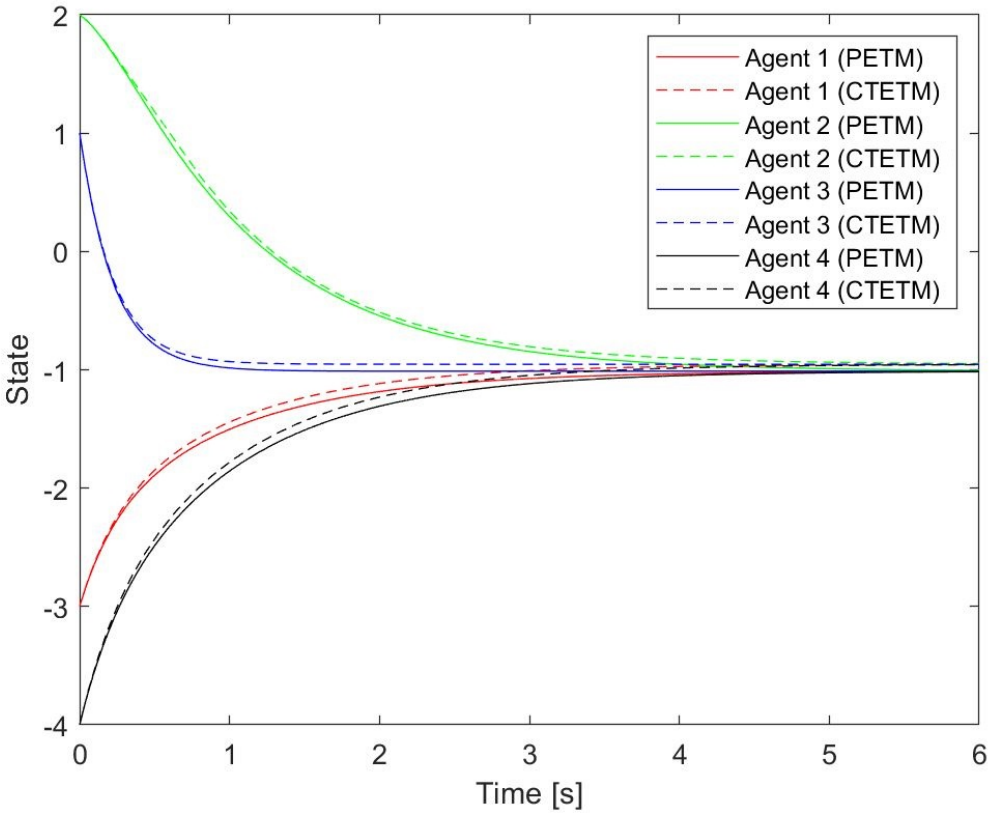

Figure 3.3: State trajectories of single-integrator agents, with Theorem 1 vs. CTETM.

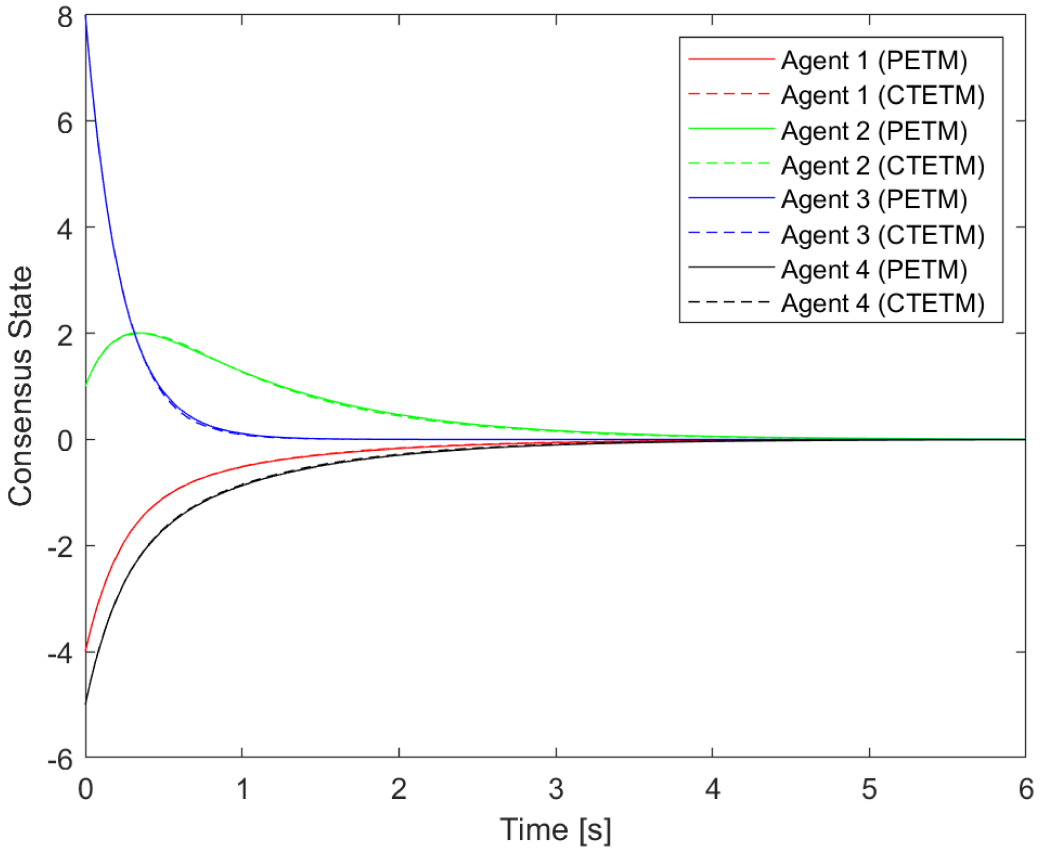

Figure 3.4: Consensus state trajectories of single-integrator agents, with Theorem 1 vs. CTETM.

Table 3.1: ETM performance comparison between dynamic PETM, according to Theorem 1, against CTETM for single-integrator agents.

Agents	Events Triggered (PETM)	Event Monitoring Instants (PETM)	Triggering Frequency (PETM)	Events Triggered (CTETM)
1	123	600	20.5%	47
2	92	800	11.5%	39
3	446	500	89.2%	2496
4	96	1200	8.0%	45

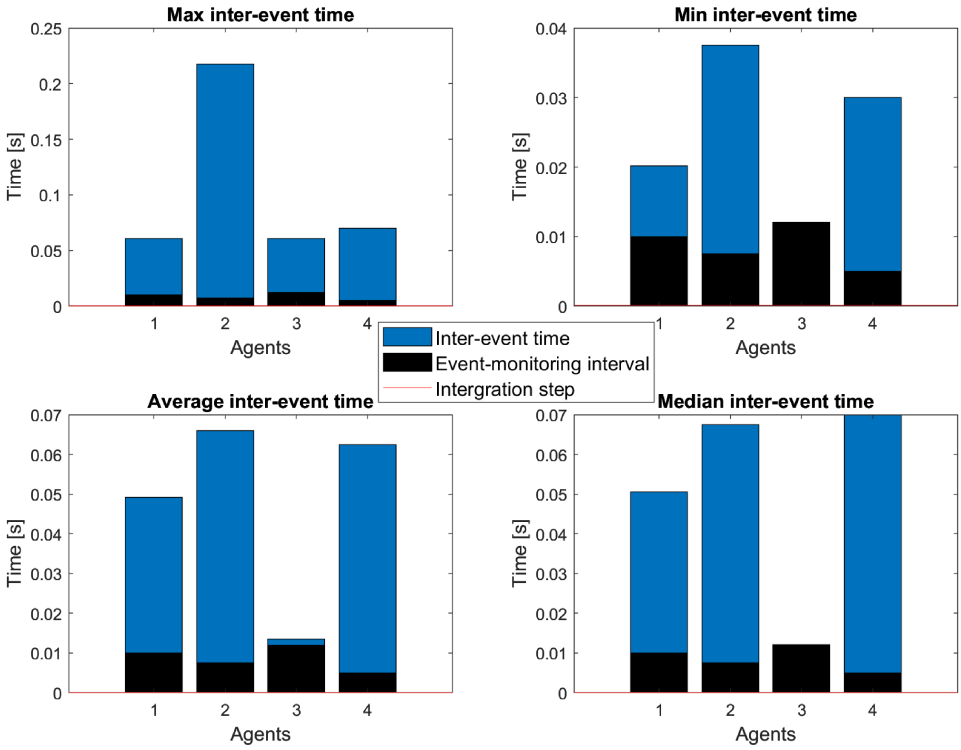

Figure 3.5: Max, min, average, and median inter-event times of single-integrator agents, with Theorem 1.

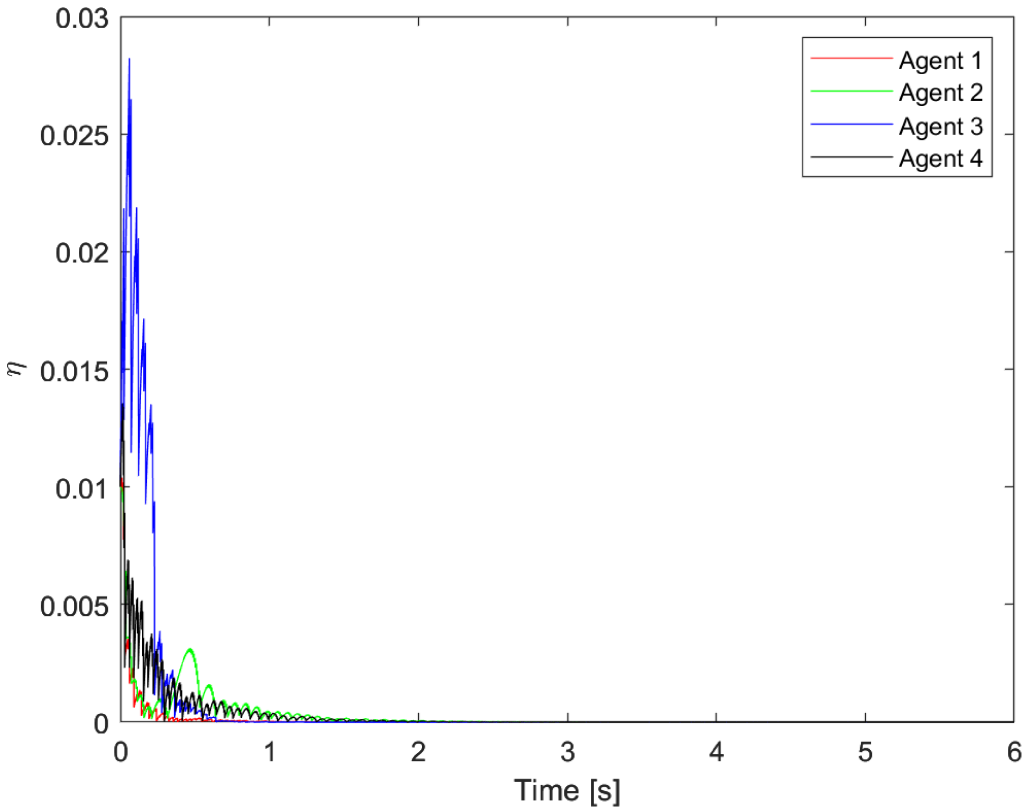

Figure 3.6: η trajectories of single-integrator agents, with Theorem 1.

Remark 6. In Figure 3.6, it can be observed that during some time intervals that η_i increases. In other words, the dynamics of η is positive. This is contributed by the $\beta_i(\hat{z}_i^T \hat{z}_i)$ component of the dynamic PETM which restrains the rate of decay, and sometimes increases, the distance of η_i from zero during flows. Through doing so, the likeliness of event occurrence at jumps reduce given the triggering condition, $g_s^i(\cdot) < 0$, in eq (2.11).

It can be seen from Table 3.1 that the total number of events triggered and EMIs, given our dynamic PETM, are 757 (column 2) and $3,100$ (column 3), respectively, while the CTETM triggered a total of $2,627$ events (column 5). Hence, the control update frequency is significantly reduced compared to a sample-data protocol, granted if control update was to occur at every EMI. As a result of our dynamic PETM protocol, the control computation and the actuator wear are significantly reduced. In addition, for this specific scenario and construction of the CTETM, the MAS employing the CTETM achieves consensus slightly faster, as seen by the trajectories in Figure 3.4, but with a higher number of events compared to our dynamic PETM (though

this is not always the case). Moreover, in the CTETM, the RSMs have to be measured continuously which: 1) is not digitally implementable, and 2) is inconsistent with the objective of reducing resource consumption. Just to highlight the second point, consider a laser diode, which commonly serves as the core component within a lidar. Let the laser diode have a power rating of 90 watts and a pulse width of 100 ns, based on the technical specification [50]. Then, sensing costs for the MAS with Theorem 1's PETM would have consumed $90\,\text{watts} \times 100\,\text{ns} \times 3,100\,\text{pulses} = 0.0279\,\text{joules}$ while $90\,\text{watts} \times 6\,\text{s} \times 4\,\text{agents} = 2160\,\text{joules}$ (hypothetically) would have been consumed with the CTETM. It evident that, comparatively, our PETM protocol presents a saving of sensing resources by $7.7 \times 10^6\%$.

Chapter 4

Linear Time-invariant MAS

In this chapter, for the system structure illustrated by Figure 3.1, our second main result fully establishes and executes the contributions listed in Section 1.4. We accomplish this by again leveraging the concepts in the preliminaries chapter and by extending the results of Chapter 3. Similar to the outline of the previous chapter, we first define our problem formulation by redefine the MAS in Section 3.1 from agents possessing single-integrator dynamics to now LTI dynamics. Then, we present our theorems that construct and establish sufficient conditions for the design of two dynamic PETMs, which we subsequently prove that consensus of the LTI MAS is guaranteed. To determine the event-monitoring intervals for the PETMs, we utilize Lemma 1 from the previous chapter to compute the MASP for each agent. Finally, we conclude this chapter by once again utilizing a numerical example to demonstrate the effectiveness of our designed protocols. Throughout this chapter, unless otherwise redefined, we maintain the same notations and definitions as were established in the previous chapters.

4.1 Problem Formulation

Consider an N-agent ($N \geq 2$) MAS coordinating over an undirected and connected interaction topology defined by $\mathcal{G} = (\mathcal{V}, \mathcal{E})$. The dynamics of each agent in the network is homogeneous and follows:

$$\dot{x}_i(t) = Ax_i(t) + Bu_i(t), \ \forall i \in \mathcal{V}, \tag{4.1}$$

where $A \in \mathbb{R}^{n\times n}$, $B \in \mathbb{R}^{n\times n_u}$, are known matrices with (A, B) *stabilizable*, and $u_i(t) \in \mathbb{R}^{n_u}$. For consensus of eq (4.1), employing RSMs and with an

event-triggered protocol, the control input for each agent $i \in \mathcal{V}$ is designed as:

$$u_i(t) = -cK\hat{z}_i(t),\ t \in [t_l^i, t_{l+1}^i), \tag{4.2}$$

where $c > 0$ is a positive constant and $K \in \mathbb{R}^{n_u \times n}$ is a constant gain matrix to be designed. Taking the same e_{ij}^i definition in accordance with eq (3.4), the agents' state dynamics in eq (4.1) and the dynamics of the stacked state vector can then be represented by:

$$\dot{x}_i = Ax_i - cBK(L_i \otimes I_n)x - cBK(\mathbf{1}_N^T \otimes I_n)e_i^i, \tag{4.3}$$

$$\dot{x} = f_x(x, e) = (I_N \otimes A)x - (L \otimes cBK)x - (I_N \otimes cBK)\tilde{I}e. \tag{4.4}$$

Furthermore, the dynamics of e_{ij}^i, given LTI agents, and the stacked vector e are given by:

$$\begin{aligned}\dot{e}_{ij}^i(t) = -a_{ij}\Big(&A\varrho_{ij} - cBK\big((L_i - L_j) \otimes I_n\big)x \\ &- cBK(\mathbf{1}_N^T \otimes I_n)(e_i^i - e_j^j)\Big),\ t \in [t_l^i, t_{l+1}^i),\end{aligned} \tag{4.5}$$

$$e_i^{i+}(t) = \begin{cases} e_i^i(t),\ t \in \{s_k^i\} \setminus \{t_l^i\}, \\ h(e_i^i(t)),\ t \in \{t_l^i\}, \end{cases} \tag{4.6}$$

$$\begin{aligned}\dot{e} = g_e(x, e) = &-\big(\mathsf{diag}(\{a_{ij}\}_{i,j\in\mathcal{V}}) \otimes A\big)\big((I_N \otimes \mathbf{1}_N - \mathbf{1}_N \otimes I_N) \otimes I_n\big)x \\ &+ \big(\mathsf{diag}(\{a_{ij}\}_{i,j\in\mathcal{V}}) \otimes cBK\big)\Big[\Big(\big((I_N \otimes \mathbf{1}_N - \mathbf{1}_N \otimes I_N)L\big) \otimes I_n\Big)x \\ &+ \big((I_N \otimes \mathbf{1}_N\mathbf{1}_N^T - \mathbf{1}_N \otimes I_N \otimes \mathbf{1}_N^T) \otimes I_n\big)e\Big].\end{aligned} \tag{4.7}$$

In this problem formulation, we again chose a dynamic PETM in order to reduce the likeliness of event occurrence. Like in Section 3.1, the dynamic PETMs follow the design framework introduced in Section 2.4 of our preliminaries chapter. The specific construction and parameter selection for consensus of the LTI MAS, eq (4.1), are detailed within our theorems under Sections 4.2 and 4.3. In addition, we continue to assume that when the ETC in eq (2.11) is satisfied, then $e_i^{i^+}(t) = h(e_i^i) = \mathbf{0}_N$, else $e_i^{i^+}(t) = e_i^i(t)$.

Similarly, we form the hybrid dynamical system for the LTI MAS by unifying the contributions of eq (2.11), eq (2.12), eq (2.13) for each agent, along with eq (4.4) and eq (4.7). We maintain the same definition of the hybrid

signal, as defined in Section 3.1, for the LTI MAS, that is, $\xi = (x, e, \tau, \eta) \in \mathbb{X} = \mathbb{R}^{nN} \times \mathbb{R}^{nN^2} \times \mathbb{R}^N_{\geq 0} \times \mathbb{R}^N_{\geq 0}$. The hybrid system, $\mathcal{H}$, can be formed by utilizing the same representations as eq (3.10) - eq (3.15). We omit explicitly stating again the expressions for $\mathcal{H}$ to avoid repetition.

The objectives for the remainder of this chapter is again to: 1) construct the dynamic PETM and establish sufficient conditions for the parameter selection, and 2) obtain the T^i for each agent in $\mathcal{V}$ such that the consensus problem is solved for the LTI MAS in eq (4.1).

4.2 Dynamic PETM Construction

In this section, we again employ the Lyapunov stability theorem to design the event-monitoring intervals governed by eq (2.10) and the dynamic PETM according to eq (2.12). Furthermore, we assume that Assumption 1, previously introduced in Section 3.2, holds, and maintain the expressions under Lemma 1 for computing the MASP for each agent. We also introduce Assumption 3 (replacing Assumption 2) and Condition 1, which combined with Assumption 1 and Lemma 1, facilitate the proof of our theorem to guarantee consensus of the LTI MAS.

To enhance clarity and reduce ambiguity, we establish some new notations and definitions that are utilized within this section. We denote $\mathscr{L} = (I_N - \frac{1}{N}\mathbf{1}_N\mathbf{1}_N^T)$ as the *average* consensus Laplacian matrix for a N-agent MAS. $\mathscr{L}$ can be interpreted analogous to L of a graph where $\mathcal{E} = \{\mathcal{V} \times \mathcal{V}\}$ and $a_{ij} = \frac{1}{N}$, for $\forall i, j \in \mathcal{V},\ i \neq j$; thereby, the properties of L for an undirected and connected graph holds for $\mathscr{L}$. Furthermore, given our problem formulation, $\mathscr{L}$ facilitates some convenient identities such as $L = \mathscr{L}L = L\mathscr{L} = \mathscr{L}L\mathscr{L}$ and $\mathscr{L} = \mathscr{L}^2$, which we exploit in this chapter. We define the average consensus state variable as $\mathfrak{z}(t) = [\mathfrak{z}_1^T(t), \cdots, \mathfrak{z}_N^T(t)]^T \in \mathbb{R}^{nN}$, where $\mathfrak{z}(t) = (\mathscr{L} \otimes I_n)x(t)$ and $\mathfrak{z}_i(t) = (\mathscr{L}_i \otimes I_n)x(t) \in \mathbb{R}^n$ with $\mathscr{L}_i$ being the i-th row of $\mathscr{L}$. Additionally, through the properties of $\mathscr{L}$, we can express $z(t) = (L \otimes I_n)\mathfrak{z}(t)$, where $\mathfrak{z} \to 0$ implies $z \to 0$. Lastly, we collectively define/denote the following:

$$\alpha = \mathsf{diag}([\alpha_1, \cdots, \alpha_N]),$$

$$\beta = \mathsf{diag}([\beta_1, \cdots, \beta_N]),$$

$$\epsilon_{\mathfrak{z}} = \mathsf{diag}([\epsilon_{\mathfrak{z}}^1, \cdots, \epsilon_{\mathfrak{z}}^N]),$$

$\epsilon_W = \mathsf{diag}([\epsilon_W^1, \cdots, \epsilon_W^N])$, where $\epsilon_{\hat{s}}^i, \epsilon_W^i \in \mathbb{R},\ \forall i \in \mathcal{V}$,

$\tilde{q} = \|I_n \otimes K^T K\|^2$,

$\tilde{q}_1 = \sum_{i,j=1}^{N} a_{ij}^2 \|cBK\big((L_i - L_j) \otimes I_n\big)\|^2$,

$\tilde{q}_\epsilon = c^2 N$,

$Q_3 = L^T \beta L$,

$\gamma = \mathsf{diag}([\gamma_1, \cdots, \gamma_N])$,

$H = [H_{11}, \cdots, H_{1N}, \cdots, H_{N1}, \cdots, H_{NN}]^T$,

$J = [J_{11}, \cdots, J_{1N}, \cdots, J_{N1}, \cdots, J_{NN}]^T$,

$\hat{z} = [\hat{z}_1^T, \cdots, \hat{z}_N^T]^T$,

$\mathcal{E}_1 \in \mathbb{R}^{N \times N}$,

$\mathcal{E}_2 \in \mathbb{R}^{N \times N}$,

$W_i^i = [(W_{i1}^i)^T, \cdots, (W_{iN}^i)^T]^T$,

$W = [(W_1^1)^T, \cdots, (W_N^N)^T]^T$,

$\tilde{\mathbf{0}}_i = [0, \cdots, 1, \cdots, 0]^T$, with 1 in the i-th element,

where $H_{ij}, J_{ij} \in \mathbb{R}_{\geq 0}$ were previously defined in Assumption 1. Next, we modify Assumption 2 to construct Assumption 3 and subsequently present Condition 1.

Assumption 3. Suppose Assumption 1 holds. Assume that for the hybrid system in Section 4.1 there exist:

- a continuous function $V(x) : \mathbb{R}^{nN} \to \mathbb{R}_{\geq 0}$,
- positive-definite function $\bar{V}^1(\cdot) : \mathbb{R}^{nN} \to \mathbb{R}_{\geq 0}$,
- positive-semi-definite function $\bar{V}^2(\cdot) : \mathbb{R}^{nN} \to \mathbb{R}_{\geq 0}$,
- positive-definite function $\bar{V}^3(\cdot) : \mathbb{R}^{nN^2} \to \mathbb{R}_{\geq 0}$,
- class $\mathcal{K}_\infty$-functions $\underline{\alpha}_V(\cdot)$, $\overline{\alpha}_V(\cdot)$,

- state transformation $\Theta(x) : \mathbb{R}^{nN} \to \mathbb{R}^{nN}$,
- function $\zeta(x), \hat{z}(x) : \mathbb{R}^{nN} \to \mathbb{R}^{nN}$,
- positive scalar σ,

such that, $W(\gamma^T\gamma \otimes I_N)W > \bar{V}^3(\cdot)$, and:

$$\underline{\alpha}_V(\|\Theta(x)\|) \leq V(x) \leq \overline{\alpha}_V(\|\Theta(x)\|), \tag{4.8}$$

$$\langle \nabla V(x), \dot{x} \rangle \leq -\bar{V}^1(\zeta) - \bar{V}^3(W) + W(\gamma^T\gamma \otimes I_N)W - \sigma H^T H - \sigma J^T J - \bar{V}^2(\hat{z}). \tag{4.9}$$

Condition 1. If (A, B) is stabilizable, then a positive-definite matrix, $P_{n\times n}$, can be found to satisfy the algebraic Riccati equation, $A^TP + PA - PBB^TP + Q = 0$, for any selection of positive-definite matrix, $Q_{n\times n}$.

Theorem 2. Let $c = \frac{1}{2\Lambda_2(L)}$ and $K = B^TP$. For $\mathcal{H}$ in Section 4.1, consider $V(x) = \frac{1}{2}x^T(\mathscr{L}^2 \otimes P)x$ and $W_{ij}^i(e_{ij}^i) = \|e_{ij}^i\|,\ \forall i, j \in \mathcal{V}$. If functions (f_η^i, g_s^i, g_t^i) of the dynamic PETM described by eq (2.12) are constructed as follows:

$$\begin{aligned} f_\eta^i &= -\alpha_i\eta_i + \beta_i(\hat{z}_i^T\hat{z}_i), \\ g_s^i &= \eta_i + \sigma\sum_{j=1}^{N}\gamma_i(\lambda_i - \frac{1}{\lambda_i} - \frac{\zeta_i}{\gamma_i})(W_{ij}^i)^2, \\ g_t^i &= \eta_i + \sigma\sum_{j=1}^{N}\gamma_i(\lambda_i - \frac{\zeta_i}{\gamma_i})(W_{ij}^i)^2, \end{aligned} \tag{4.10}$$

where $\zeta_i > 0$ is a small arbitrary constant, and the design parameters $\alpha_i > 0$, $\beta_i \geq 0$, $\epsilon_\zeta^i > 0$, $\epsilon_W^i > 0$, $\forall i \in \mathcal{V}$, $\sigma > 0$, $\sigma_1 > 0$, and $Q > 0$ are such that:

$$Q_1 = \Big(\big(\Lambda_m(Q) - \sigma_1\tilde{q} - 16\sigma\|A\|^2a_{max}^2N - 4\sigma\tilde{q}_1\big)I_N - 2\epsilon_\zeta\Big) \geq 0,$$

$$\mathcal{E}_1 = (\epsilon_\zeta - 2Q_3) > 0,$$

$$\mathcal{E}_2 = (\varepsilon_W - 2N\beta) > 0.$$

And with T^i computed through Lemma 1 using:

$$C_{ij} = a_{ij}c\|BK\|,$$

$$\gamma_i = \tilde{\mathbf{0}}_i^T\sqrt{\gamma^T\gamma}\tilde{\mathbf{0}}_i, \quad \text{for } \gamma^T\gamma = (\tfrac{\tilde{q}_\epsilon}{2\sigma_1} + 4\sigma a_{max}^2c^2\|BK\|^2N^2)I_N + \epsilon_W,$$

then the closed-loop system is asymptotically stable with respect to $\{x \in \mathbb{R}^{nN} | \big(M\Lambda(\mathscr{L})M^T \otimes \sqrt{(P)}\big)x = 0\}$ (stabilizing set for consensus of the LTI MAS).

Remark 7. In Theorem 2, it can be observed that the system A matrix influences the parameter selection for the dynamic PETM, thus affecting its performance. Intuitively, when the agents are more dynamic (i.e., the eigenvalues of the system matrix are father away from the origin on the real and imaginary plane), then it is expected that the PETM must check for events more frequently to account for the potentially rapid changes in system states. This intuition holds true within our theorem because when the maximum eigenvalue of A is large, a smaller σ is required to counteract the contributions of A to satisfy the condition $Q_1 \geq 0$. We can see from eq (3.20) that a smaller σ results in the dynamics of $\theta_i(t)$ being more negative. As a consequence, the time it takes for $\theta_i(t)$ to evolve from $\theta_i(0)$ to $\theta_i(T^i)$ is shorter; hence, the MASP of the PETM is smaller, contributing to more frequent EMIs.

Proof. Similar to the proof in Section 3.2, we show that with the specific form of W_{ij}^i, $V(x)$, and conditions on the construction of the dynamic PETM, presented under Theorem 2, that Assumptions 1 and 3 are satisfied. Subsequently, we show that consensus of the LTI MAS is achieved using the previously introduced hybrid system Lyapunov function, eq (3.24).

Checking Assumption 1. Again, for $W_{ij}^i = \|e_{ij}^i\|$, W_{ij}^i can be lower and upper bounded by $\mathcal{K}_\infty$ functions via scalar constants. To upper bound the error growth rate, we employ the dynamics of $e_{ij}^i(t)$ defined by eq (4.5). Then:

$$\begin{aligned}
\langle \nabla W_{ij}^i(e_{ij}^i),\ \dot{e}_{ij}^i \rangle &= \frac{\langle e_{ij}^i, \dot{e}_{ij}^i \rangle}{\|e_{ij}^i\|} && (4.11)\\
&\leq \|\dot{e}_{ij}^i\|, && (4.12)\\
&\leq \|-a_{ij}\Big(A\varrho_{ij} - cBK\big((L_i - L_j) \otimes I_n\big)x && (4.13)\\
&\quad - cBK(\mathbf{1}_N^T \otimes I_n)(e_i^i - e_j^j)\Big)\|,\\
&\leq \|a_{ij}\Big(A\varrho_{ij} - cBK\big((L_i - L_j) \otimes I_n\big)x\Big)\| && (4.14)\\
&\quad + \|a_{ij}cBK(\mathbf{1}_N^T \otimes I_n)e_i^i\| + \|a_{ij}cBK(\mathbf{1}_N^T \otimes I_n)e_j^j\|,
\end{aligned}$$

which by employing series of norm inequalities, and the fact that $\|a_{ij}cBK(\mathbf{1}_N^T \otimes$

$I_n)e_i^i\| \leq a_{ij}c\|BK\|\mathbf{1}_N^T W_i^i$, leads to:

$$\langle \nabla W_{ij}^i(e_{ij}^i),\ \dot{e}_{ij}^i \rangle \leq \underbrace{a_{ij}c\|BK\|W_{ij}^i}_{C_{ij}W_{ij}^i} + \underbrace{a_{ij}\|A\varrho_{ij} - cBK((L_i - L_j)\otimes I_n)x\|}_{H_{ij}} + \underbrace{a_{ij}c\|BK\|(\mathbf{1}_N^T - \tilde{\mathbf{0}}_j^T)W_i^i + a_{ij}c\|BK\|\mathbf{1}_N^T W_j^j}_{J_{ij}}. \tag{4.15}$$

With the above, Assumption 1 is verified. Next we check Assumption 2.

Checking Assumption 3. As previously mentioned, $\mathscr{L}$ can be interpreted as a Laplacian matrix of a N-node graph where $\mathcal{E} = \{\mathcal{V} \times \mathcal{V}\}$; therefore, the properties for an undirected and connected graph apply. Hence, we diagonalize $\mathscr{L} = M\Lambda(\mathscr{L})M^T$ and take the new stabilizing set as $\Theta(x) = \big(M\Lambda(\mathscr{L})M^T \otimes \sqrt{(P)}\big)x$ where we can again express $V(x) = \frac{1}{2}\|\Theta(x)\|^2$. As $\Lambda_1(\mathscr{L}) = 0$, there exists an $x \neq 0$ such that $\Theta(x) = 0$. Furthermore, it is clear to see that $V(x)$ can be lower and upper bounded by $\underline{\alpha}_V(\|\Theta(x)\|)$ and $\overline{\alpha}_V(\|\Theta(x)\|)$ through scalar constants. Next, we can express $\dot{V}$ as:

$$\begin{aligned}
\langle \nabla V(x), \dot{x}\rangle &= \frac{1}{2}\dot{x}^T(\mathscr{L}^2 \otimes P)x + \frac{1}{2}x^T(\mathscr{L}^2 \otimes P)\dot{x}, \\
&= \frac{1}{2}x^T(I_N \otimes A)^T(\mathscr{L}^2 \otimes P)x + \frac{1}{2}x^T(\mathscr{L}^2 \otimes P)(I_N \otimes A)x \\
&\quad - x^T(\mathscr{L}^2 \otimes P)(L \otimes cBK)x - x^T(\mathscr{L}^2 \otimes cPBK)\tilde{I}e, \\
&= \frac{1}{2}x^T(\mathscr{L} \otimes I_n)^T\Big(\big(I_N \otimes (A^TP + PA)\big) - 2(L \otimes cPBK)\Big) \\
&\quad (\mathscr{L} \otimes I_n)x - x^T(\mathscr{L}^2 \otimes cPBK)\tilde{I}e.
\end{aligned} \tag{4.16}$$

By substituting the average consensus variable $\mathfrak{z}(t) = (\mathscr{L}\otimes I_n)x(t)$, $c = \frac{1}{2\Lambda_2(L)}$, the fact that $\Lambda_2(L)\|\mathfrak{z}\|^2 \leq \mathfrak{z}^T L\mathfrak{z}$ (proof omitted), and utilizing Condition 1, we can upper bound the first term on the right-hand side of eq (4.16) as:

$$\begin{aligned}
&\frac{1}{2}x^T(\mathscr{L} \otimes I_n)^T\Big(\big(I_N \otimes (A^TP + PA)\big) - 2(L \otimes cPBK)\Big)(\mathscr{L} \otimes I_n)x \\
&\qquad \leq \frac{1}{2}\mathfrak{z}^T\Big(I_N \otimes (A^TP + PA - PBB^TP)\Big)\mathfrak{z}, \\
&\qquad \leq -\frac{1}{2}\mathfrak{z}^T\Big(I_N \otimes \Lambda_m(Q)I_n\Big)\mathfrak{z} < 0.
\end{aligned} \tag{4.17}$$

For the second terms on the right-hand side of eq (4.16), we utilize Young's inequality to separate the cross-terms and use the fact that $\mathscr{L} = \mathscr{L}^2$ to obtain the upper bound:

$$-x^T(\mathscr{L}^2 \otimes cPBK)\tilde{I}e \leq \frac{\sigma_1}{2}\mathfrak{z}^T(I_N \otimes \tilde{q}I_n)\mathfrak{z} + \frac{\tilde{q}_\epsilon}{2\sigma_1}W^TW. \tag{4.18}$$

Employing eq (4.17) and eq (4.18), we can obtain:

$$\langle \nabla V(x), \dot{x} \rangle \leq -\frac{1}{2}\mathfrak{z}^T \Big(I_N \otimes \big(\Lambda_m(Q) - \sigma_1 \tilde{q} \big) I_n \Big) \mathfrak{z} + \frac{\tilde{q}_\epsilon}{2\sigma_1} W^T W. \tag{4.19}$$

We then add and subtract the terms: $\mathfrak{z}^T(\epsilon_\mathfrak{z} \otimes I_n)\mathfrak{z}$, $W^T(\epsilon_W \otimes I_N)W$, $\sigma H^T H$, $\sigma J^T J$ to eq (4.19). Utilizing norm inequalities and the identity $\varrho_{ij} = (x_i - x_j) = (x_i - x_j - \frac{1}{N}\mathbf{1}_N^T x + \frac{1}{N}\mathbf{1}_N^T x) = (\mathfrak{z}_i - \mathfrak{z}_j)$, the latter two terms can be upper bounded by:

$$\sigma H^T H \leq \frac{1}{2}\mathfrak{z}^T \big(I_N \otimes (16\sigma \|A\|^2 a_{max}^2 N + 4\sigma \tilde{q}_1) I_n \big) \mathfrak{z}, \tag{4.20}$$

$$\sigma J^T J \leq 4\sigma a_{max}^2 c^2 \|BK\|^2 N^2 W^T W. \tag{4.21}$$

Incorporating eq (4.20) and eq (4.21) into eq (4.19) for $\sigma H^T H$ and $\sigma J^T J$, we have:

$$\begin{aligned}
\langle \nabla V(x), \dot{x} \rangle \leq & -\mathfrak{z}^T(\epsilon_\mathfrak{z} \otimes I_n)\mathfrak{z} - W^T(\epsilon_W \otimes I_N)W \\
& - \frac{1}{2}\mathfrak{z}^T \Big(\underbrace{\big((\Lambda_m(Q) - \sigma_1 \tilde{q} - 16\sigma \|A\|^2 a_{max}^2 N - 4\sigma \tilde{q}_1) I_N - 2\epsilon_\mathfrak{z} \big)}_{Q_1} \otimes I_n \Big) \mathfrak{z} \\
& + W^T \Big(\underbrace{\big((\frac{\tilde{q}_\epsilon}{2\sigma_1} + 4\sigma a_{max}^2 c^2 \|BK\|^2 N^2) I_N + \epsilon_W \big)}_{\gamma^T \gamma} \otimes I_N \Big) W \\
& - \sigma H^T H - \sigma J^T J.
\end{aligned} \tag{4.22}$$

Since we select parameters in accordance with Theorem 2 such that $Q_1 \geq 0$, then:

$$\begin{aligned}
\langle \nabla V(x), \dot{x} \rangle \leq & -\mathfrak{z}^T(\epsilon_\mathfrak{z} \otimes I_n)\mathfrak{z} - W^T(\epsilon_W \otimes I_N)W \\
& + W^T(\gamma^T \gamma \otimes I_N)W - \sigma H^T H - \sigma J^T J.
\end{aligned} \tag{4.23}$$

We then add and subtract $\hat{z}(\beta \otimes I_n)\hat{z}$ (contribution from the dynamic PETM) to eq (4.23) where its upper bound is:

$$\hat{z}(\beta \otimes I_n)\hat{z} \leq \mathfrak{z}^T(2Q_3 \otimes I_n)\mathfrak{z} + W^T(2N\beta \otimes I_N)W. \tag{4.24}$$

With eq (4.24), we arrive at the upper bound for $\dot{V}$ as:

$$\begin{aligned}
\langle \nabla V(x), \dot{x} \rangle \leq & -\mathfrak{z}^T \big(\underbrace{(\epsilon_\mathfrak{z} - 2Q_3)}_{\mathcal{E}_1} \otimes I_n \big) \mathfrak{z} - W^T \big(\underbrace{(\epsilon_W - 2N\beta)}_{\mathcal{E}_2} \otimes I_N \big) W \\
& + W^T(\gamma^T \gamma \otimes I_N)W - \sigma H^T H - \sigma J^T J - \hat{z}(\beta \otimes I_n)\hat{z}.
\end{aligned} \tag{4.25}$$

Since we also select parameters, in accordance with Theorem 2, such that $\mathcal{E}_1, \mathcal{E}_2 > 0$, and $\beta \geq 0$, then:

$$\begin{aligned}\langle \nabla V(x), \dot{x} \rangle \leq & -\underbrace{\mathfrak{z}^T(\mathcal{E}_1 \otimes I_n)\mathfrak{z}}_{\bar{V}^1(\cdot)} - \underbrace{W^T(\mathcal{E}_2 \otimes I_N)W}_{\bar{V}^3(\cdot)} \\ & + W^T(\gamma^T\gamma \otimes I_N)W - \sigma H^T H - \sigma J^T J - \underbrace{\hat{z}^T(\beta \otimes I_n)\hat{z}}_{\bar{V}^2(\cdot)},\end{aligned} \tag{4.26}$$

with which Assumption 2 is satisfied. Next, we will show that consensus for the LTI MAS employing Theorem 2's PETM is guaranteed. For $\mathcal{H}$, established in Section 4.1, with the hybrid system Lyapunov function, defined in eq (3.24), we again need to show that $U(\xi)$ monotonically decreases over both the flow domain, C, and jump domain, D.

Flow domain. During the flow domain, the time derivative of $U(\xi)$ is represented by eq (3.34). We substitute eq (3.20), eq (4.10), eq (4.15), and eq (4.26) for the associated time derivatives on the right-hand side of eq (3.34), yielding:

$$\begin{aligned}\dot{U} \leq & -\mathfrak{z}^T(\mathcal{E}_1 \otimes I_n)\mathfrak{z} - W^T(\mathcal{E}_2 \otimes I_N)W \\ & + W^T(\gamma^T\gamma \otimes I_N)W - \sigma H^T H - \sigma J^T J - \hat{z}^T(\beta \otimes I_n)\hat{z} \\ & + \sigma \sum_{i,j=1}^{N} \gamma_i(-2\gamma_i\theta_i^2 - 2C_i\theta_i - \frac{1}{\sigma}\gamma_i)(W_{ij}^i)^2 \\ & + 2\sigma \sum_{i,j=1}^{N} \gamma_i\theta_i W_{ij}^i(C_{ij}W_{ij}^i + H_{ij} + J_{ij}) \\ & + \mathbf{1}_N^T\Big(- \alpha\eta + \beta\mathsf{blkdiag}(\{z_1^T, \cdots, z_N^T\})\hat{z}\Big).\end{aligned} \tag{4.27}$$

We again separate the cross-terms to obtain:

$$\begin{aligned}2\sigma \sum_{i,j=1}^{N} \gamma_i\theta_i W_{ij}^i(C_{ij}W_{ij}^i + H_{ij} + J_{ij}) \leq & \\ 2\sigma \sum_{i,j=1}^{N} \gamma_i\theta_i C_i(W_{ij}^i)^2 + 2\sigma \sum_{i,j=1}^{N} (\gamma_i\theta_i W_{ij}^i)^2 + \sigma H^T H + \sigma J^T J.&\end{aligned} \tag{4.28}$$

We substitute eq (4.28) into eq (4.27) and after cancelling like terms, we obtain:

$$\dot{U} \leq -\mathfrak{z}^T(\mathcal{E}_1 \otimes I_n)\mathfrak{z} - W^T(\mathcal{E}_2 \otimes I_N)W - \mathbf{1}_N^T\alpha\eta. \tag{4.29}$$

Since $\mathscr{E}_1, \mathscr{E}_2, \alpha > 0$, from Theorem 2, we have:

$$\dot{U}(\xi) \leq -\psi(U(\xi)),\ \forall \xi \in C, \tag{4.30}$$

with which it is shown that $U(\xi)$ monotonically decreases over the flow domain, C.

Jump domain. To show that $U(\xi)$ monotonically decreases over the jump domain, D, we need to show that the Lyapunov function candidate decreases after each jump. We maintain the set definitions for Γ, Ψ, Φ, Ω according to eq (3.39) - eq (3.42). Then, we can similarly partition $U(\xi)$ into eq (3.43). Again applying the fact that $\tau_i \leq T^i \rightarrow \theta_i(\tau_i) \geq \theta_i(T^i) = \lambda_i$ (or $-\theta_i(\tau_i) \leq -\lambda_i$), and $x^+ = x$ at jumps, we have:

$$\sigma \sum_{i\in\Gamma\cup\Phi_t} \sum_{j=1}^{N} \gamma_i \theta_i^+ (W_{ij}^{i^+})^2 + \sum_{i\in\Gamma\cup\Phi_t} \eta_i^+ = \sum_{i\in\Gamma\cup\Phi_t} (\eta_i + \sigma \sum_{j=1}^{N} \gamma_i (\lambda_i - \frac{\delta_i}{\gamma_i})(W_{ij}^i)^2), \tag{4.31}$$

and:

$$\sigma \sum_{i\in\Psi\cup\Phi_s} \sum_{j=1}^{N} \gamma_i \theta_i^+ (W_{ij}^{i^+})^2 + \sum_{i\in\Psi\cup\Phi_s} \eta_i^+ = \sigma \sum_{i\in\Psi\cup\Phi_s} \sum_{j=1}^{N} \gamma_i (\frac{1}{\lambda_i})(W_{ij}^i)^2 + \sum_{i\in\Psi\cup\Phi_s} (\eta_i + \sigma \sum_{j=1}^{N} \gamma_i (\lambda_i - \frac{1}{\lambda_i} - \frac{\delta_i}{\gamma_i})(W_{ij}^i)^2), \tag{4.32}$$

and:

$$\sigma \sum_{i\in\Omega} \sum_{j=1}^{N} \gamma_i \theta_i^+ (W_{ij}^{i^+})^2 + \sum_{i\in\Omega} \eta_i^+ = \sigma \sum_{i\in\Omega} \sum_{j=1}^{N} \gamma_i \theta_i (W_{ij}^i)^2 + \sum_{i\in\Omega} \eta_i. \tag{4.33}$$

Performing the same set partition on $U(\xi)$, then we obtain the inequality:

$$U(\xi^+) - U(\xi) \leq -\sigma \sum_{i\in\Gamma\cup\Phi_t} \sum_{j=1}^{N} \delta_i (W_{ij}^i)^2 - \sigma \sum_{i\in\Theta\cup\Phi_s} \sum_{j=1}^{N} \delta_i (W_{ij}^i)^2. \tag{4.34}$$

As $\sigma > 0$ and $\delta_i > 0$, according to Theorem 2, then:

$$U(\xi^+) - U(\xi) \leq 0, \tag{4.35}$$

with which it is shown that $U(\xi)$ monotonically decreases after jumps.

Combining eq (4.30) and eq (4.35), the proof is complete and asymptotic consensus of the LTI MAS, eq (4.1), with the control protocol, eq (4.2), and dynamic PETM, in accordance with Theorem 2, is guaranteed. Later in Section 4.4, we verify the results of this section as well as the performance of Theorem 2's PETM with a numerical example.

4.3 Dynamic PETM Construction Incorporating an Independently Tunable Time-dependent Function

In this section, for the hybrid system $\mathcal{H}$ formulated in Section 4.1, we extend the results of Section 4.2 by modifying the construction of Theorem 2's PETM. This modification aims to provide more design flexibility and improve ETM performance while still guaranteeing consensus of the LTI MAS. The modification to Theorem 2's PETM follows incorporating an exponential decay term (time-based threshold) into f_η^i. The purpose of the exponential term is analogous to the contribution from $\beta_i(\hat{z}_i^T\hat{z}_i)$ regarding event frequency, as mentioned in Remark 3. The caveat of incorporating such a time-based threshold has been mentioned in Subsection 1.2.2. The computation of T^i remains unchanged from Section 4.2.

Theorem 3. Let $c = \frac{1}{2\Lambda_2(L)}$ and $K = B^TP$. For $\mathcal{H}$ in Section 4.1, consider $V(x) = \frac{1}{2}x^T(\mathscr{L}^2 \otimes P)x$ and $W_{ij}^i(e_{ij}^i) = \|e_{ij}^i\|,\ \forall i,j \in \mathcal{V}$. If functions (f_η^i, g_s^i, g_t^i) of the dynamic PETM described by eq (2.12) are as follows:

$$\begin{aligned} f_\eta^i &= -\alpha_i\eta_i + \beta_i(\hat{z}_i^T\hat{z}_i) + \delta_1^i e^{-\delta_2^i t}, \\ g_s^i &= \eta_i + \sigma\sum_{j=1}^{N}\gamma_i(\lambda_i - \frac{1}{\lambda_i} - \frac{\zeta_i}{\gamma_i})(W_{ij}^i)^2, \\ g_t^i &= \eta_i + \sigma\sum_{j=1}^{N}\gamma_i(\lambda_i - \frac{\zeta_i}{\gamma_i})(W_{ij}^i)^2, \end{aligned} \tag{4.36}$$

where $\zeta_i > 0$ is a small arbitrary constant, $\delta_1^i \geq 0$, $\delta_2^i > 0$, and the design parameters $\alpha_i > 0$, $\beta_i \geq 0$, $\epsilon_{\dot{z}}^i > 0$, $\epsilon_W^i > 0$, $\forall i \in \mathcal{V}$, $\sigma > 0$, $\sigma_1 > 0$, and $Q > 0$ are such that:

$$Q_1 = \Big(\big(\Lambda_m(Q) - \sigma_1\tilde{q} - 16\sigma\|A\|^2a_{max}^2N - 4\sigma\tilde{q}_1\big)I_N - 2\epsilon_{\dot{z}}\Big) \geq 0,$$

$$\mathcal{E}_1 = (\epsilon_{\dot{z}} - 2Q_3) > 0,$$

$$\mathcal{E}_2 = (\varepsilon_W - 2N\beta) > 0,$$

And with T^i computed through Lemma 1 using:

$$C_{ij} = a_{ij}c\|BK\|,$$
$$\gamma_i = \tilde{\mathbf{0}}_i^T \sqrt{\gamma^T\gamma}\tilde{\mathbf{0}}_i, \quad \text{for } \gamma^T\gamma = (\tfrac{\tilde{q}_\epsilon}{2\sigma_1} + 4\sigma a_{max}^2 c^2\|BK\|^2N^2)I_N + \epsilon_W,$$

then the closed-loop system is asymptotically stable with respect to $\{x \in \mathbb{R}^{nN} | \big(M\Lambda(\mathscr{L})M^T \otimes \sqrt{(P)}\big)x = 0\}$ (stabilizing set for consensus of the LTI MAS).

Remark 8. It can be seen that as $t \to \infty$, $\delta_1^i e^{-\delta_2^i t} \to 0$, $\forall i \in \mathcal{V}$. Therefore, as $t \to \infty$, the construction of Theorem 3's PETM approaches Theorem 2's PETM, which we have proven guarantees consensus for the LTI MAS eq (4.1).

Proof. Since we only incorporate an exponential decay term into f_η^i of each agent, the consensus proof of Section 4.2 remains largely the same. The only change from Section 4.2 is in the "*Flow domain*" step. As the other steps of the proof remain unaffected by the incorporation of the exponential decay term, we choose to omit those steps in this proof to avoid repetition.

Flow domain. Given $\dot{\eta}_i = f_\eta^i$, where f_η^i is from Theorem 3, we can simply modify eq (4.29) to:

$$\dot{U} \leq -\zeta^T(\mathcal{E}_1 \otimes I_n)\zeta - W^T(\mathcal{E}_2 \otimes I_N)W - \mathbf{1}_N^T\alpha\eta + \sum_{i=1}^{N} \delta_1^i e^{-\delta_2^i t}. \tag{4.37}$$

As a result of the sum of exponential term, it is difficult to express $\dot{U}(\xi) \leq -\psi(U(\xi)),\ \forall \xi \in C$. Instead, we employ Barbalet's lemma introduced in Section 2.5 to show that as $t \to \infty$ that $\dot{U}, \zeta, W, \eta \to 0$. In order to do so, we need to show that:

$$\lim_{t\to\infty} \int_0^t \dot{U} dt \leq K_1, \tag{4.38}$$

$$\lim_{t\to\infty} \int_0^t \big(\zeta^T\zeta + W^TW + \mathbf{1}_N^T\eta\big)dt \leq K_2, \tag{4.39}$$

where $|K_1|, |K_2| < \infty$ are arbitrary finite constants. To show eq (4.38), we use the fact that $\mathcal{E}_1, \mathcal{E}_2, \alpha > 0$ where we can upper bound eq (4.37) by just:

$$\dot{U} \leq \sum_{i=1}^{N} \delta_1^i e^{-\delta_2^i t}. \tag{4.40}$$

Integrating both sides from 0 to t and taking the limit as $t \to \infty$, we can see that:

$$\begin{aligned} U(\infty) - U(0) &\leq \sum_{i=1}^{N} \frac{\delta_1^i}{\delta_2^i}, \\ &\leq K_1. \end{aligned} \tag{4.41}$$

Thus, with the above, in accordance with Barbalat's lemma we can claim that $\dot{U} \to 0$ as $t \to \infty$ and that ζ, W, η are at least bounded. To show eq (4.39), we first define $\bar{\Lambda}_m = \mathsf{min}\{\Lambda_m(\mathcal{E}_1), \Lambda_m(\mathcal{E}_2), \Lambda_m(\alpha)\}$. Then we can establish an upper bound to eq (4.37) as:

$$\dot{U} \leq -\bar{\Lambda}_m \zeta^T \zeta - \bar{\Lambda}_m W^T W - \bar{\Lambda}_m \mathbf{1}_N^T \eta + \sum_{i=1}^{N} \delta_1^i e^{-\delta_2^i t}, \tag{4.42}$$

which we can rearrange as:

$$\zeta^T \zeta + W^T W + \mathbf{1}_N^T \eta \leq -\frac{1}{\bar{\Lambda}_m} \dot{U} + \frac{1}{\bar{\Lambda}_m} \sum_{i=1}^{N} \delta_1^i e^{-\delta_2^i t}. \tag{4.43}$$

Integrating both sides from 0 to t and taking the limit as $t \to \infty$, we obtain:

$$\lim_{t \to \infty} \int_0^t (\zeta^T \zeta + W^T W + \mathbf{1}_N^T \eta) dt \leq -\frac{1}{\bar{\Lambda}_m} \underbrace{\big(U(\infty) - U(0)\big)}_{\leq K_1} + \frac{1}{\bar{\Lambda}_m} \sum_{i=1}^{N} \frac{\delta_1^i}{\delta_2^i}, \tag{4.44}$$

$$\leq K_2. \tag{4.45}$$

Again according to Barbalat's lemma, $\zeta, W, \eta \to 0$ as $t \to \infty$. Combined with the jump domain proof of Section 4.2, consensus of the LTI MAS, eq (4.1), with Theorem 3's PETM, is guaranteed. This concludes the proof. In the subsequent numerical example, we verify the results of this section.

4.4 Numerical Example

In this section, we consider a numerical example involving a 4-agent MAS coordinating under the same graph $\mathcal{G}$ as in Section 3.3. As a consequence, the Laplacian matrix representing $\mathcal{G}$ is again expressed by eq (3.49). Each agent's dynamics is modelled by eq (4.1) where we've selected the system matrices as:

$$A = \begin{bmatrix} 0 & 2 \\ -3 & 0 \end{bmatrix}, \quad B = \begin{bmatrix} 0 \\ 1 \end{bmatrix}, \tag{4.46}$$

and with the control input protocol following eq (4.2). It can be seen through the A matrix that the agents exhibit purely harmonic behaviour; thus, trivial consensus through stabilization to the origin is avoided. As well, given eq (4.46), it can be determined that (A, B) is controllable. For this example, we select the following design parameters:

$$c = \frac{1}{2\Lambda_2(L)}, \tag{4.47}$$

$$K = B^T P, \tag{4.48}$$

$$Q = \mathsf{diag}([0.5, 0.5]), \tag{4.49}$$

$$\epsilon_{\dot{s}} = \mathsf{diag}([0.05, 0.1, 0.15, 0.15]), \tag{4.50}$$

$$\epsilon_W = \mathsf{diag}([0.05, 0.1, 0.15, 0.15]), \tag{4.51}$$

$$\alpha = \mathsf{diag}([0.04, 0.03, 0.02, 0.01]), \tag{4.52}$$

$$\beta = \mathsf{diag}([0.0027, 0.0022, 0.0032, 0.015]), \tag{4.53}$$

$$[\zeta_1, \zeta_2, \zeta_3, \zeta_4] = [0.0284, 0.08, 0.0824, 0.1244], \tag{4.54}$$

$$\sigma_1 = \frac{1}{22\tilde{q}}, \tag{4.55}$$

$$\sigma = \frac{1}{22(16\|A\|^2 a_{max}^2 N + \tilde{q}_1)}, \tag{4.56}$$

$$[\lambda_1, \lambda_2, \lambda_3, \lambda_4] = [0.02, 0.015, 0.03, 0.01]. \tag{4.57}$$

According to the theorems in this chapter, we obtain:

$$Q_1 = \mathsf{diag}([0.3091, 0.2091, 0.1091, 0.1091]), \tag{4.58}$$

$$\mathcal{E}_1 = \begin{bmatrix} 0.0382 & -0.0064 & 0.0246 & -0.0064 \\ -0.0064 & 0.0892 & 0.0236 & -0.0064 \\ 0.0246 & 0.0236 & 0.0526 & 0.0492 \\ -0.0064 & -0.0064 & 0.0492 & 0.1136 \end{bmatrix}, \tag{4.59}$$

$$\mathcal{E}_2 = \mathsf{diag}([0.0284, 0.0824, 0.1244, 0.030]), \tag{4.60}$$

$$\gamma^T \gamma = \mathsf{diag}([7.7311, 7.7811, 7.8311, 7.8311]). \tag{4.61}$$

It can be seen that with our parameter selection, the eigenvalues of $Q_1, \mathcal{E}_1, \mathcal{E}_2 > 0$, thus, indicating positive-definiteness. Following Lemma 1, we calculate the T^is for the agents as:

$$[T^1, T^2, T^3, T^4] = [0.0011, 0.0014, 0.0008, 0.0018]. \tag{4.62}$$

Here, due to the contrast in our selection of λ_i, the computed T^i has greater distinction between one another. For the simulation, we select the asynchronous periodic event-monitoring intervals for the agents as $[(s_{k+1}^i - s_k^i)]_{\forall i \in \mathcal{V}} =$

$[T^1, T^2, T^3, T^4]$. Additionally, we simulate the CTETM, designed in [19], to compare with our results for the same LTI MAS. For our simulation, we utilize an integration time step of 1×10^{-5} seconds.

4.4.1 Simulation 1

In this subsection we present the simulation results for the LTI MAS utilizing Theorem 2's PETM with parameter selection as described in Section 4.4. Since $Q_1, \mathcal{E}_1, \mathcal{E}_2 > 0$ and the event-monitoring intervals for each agent is less than or equal to T^i for all time, consensus of the LTI MAS, employing Theorem 2's PETM, is guaranteed through the proof of Subsection 4.2. Figure 4.1 presents the state trajectories of each agent in the MAS, where the states can be seen converging. Figure 4.2 presents the average consensus state trajectory $\bar{z}(t)$, which can be seen approaching the origin, thus clearly achieving consensus. We again note the relationship $z(t) = (L \otimes I_n)\bar{z}(t)$, where $\bar{z}(t) \to 0$ implies $z(t) \to 0$. Table 4.1 summarizes the event-trigger frequencies for both Theorem 2's PETM and the CTETM. Figure 4.3 plots the trajectories of the auxiliary PETM variable η. Lastly, Figure 4.4 provides some statistical data with respect to the inter-event times for Theorem 2's PETM.

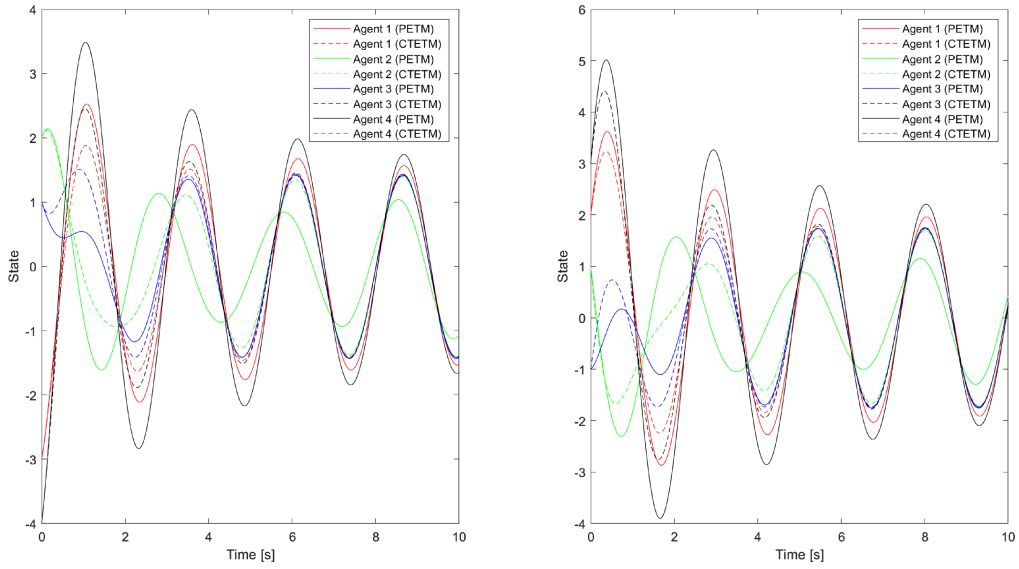

Figure 4.1: 1st (left) and 2nd (right) state trajectories of LTI agents, with Theorem 2 vs. CTETM.

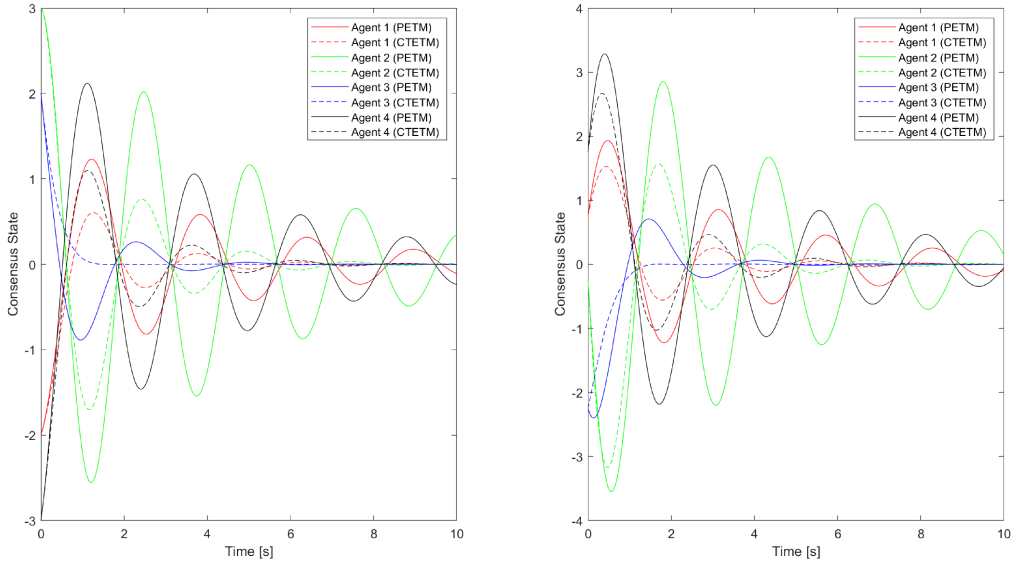

Figure 4.2: 1st (left) and 2nd (right) average consensus state trajectories of LTI agents, with Theorem 2 vs. CTETM.

Table 4.1: ETM performance comparison between dynamic PETM, according to Theorem 2, against CTETM for LTI agents.

Agents	Events Triggered (PETM)	Event Monitoring Instants (PETM)	Triggering Frequency (PETM)	Events Triggered (CTETM)
1	739	9252	7.9%	1762
2	884	7404	11.9%	2841
3	7418	13282	55.8%	408
4	359	5681	6.3%	1055

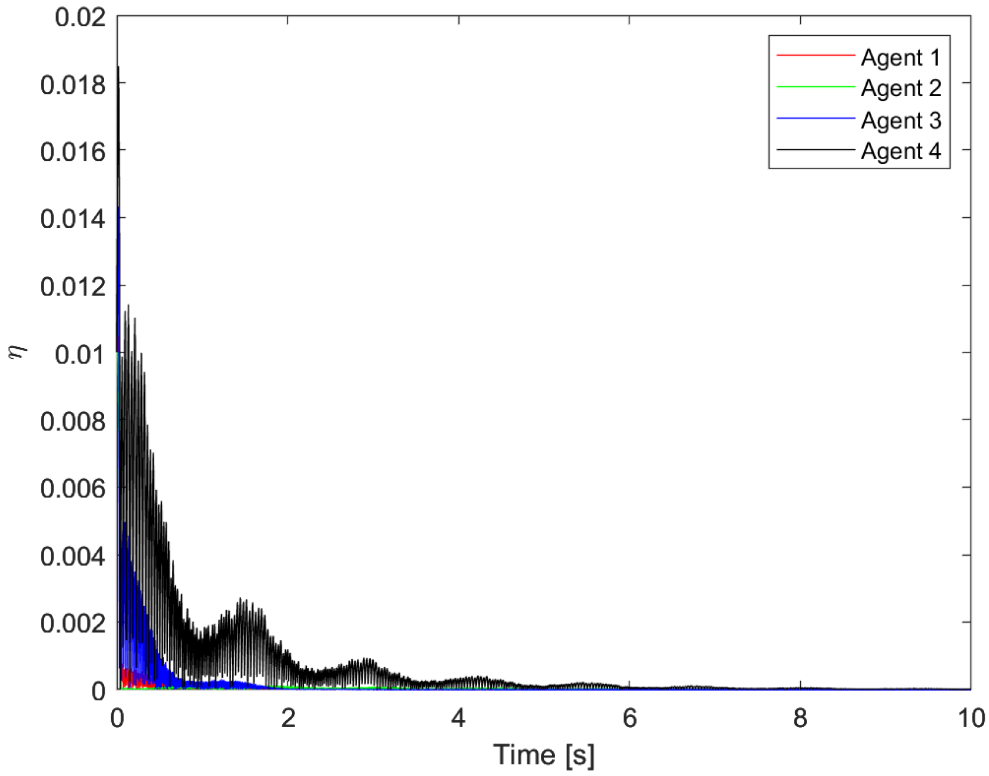

Figure 4.3: η trajectories of LTI agents, with Theorem 2.

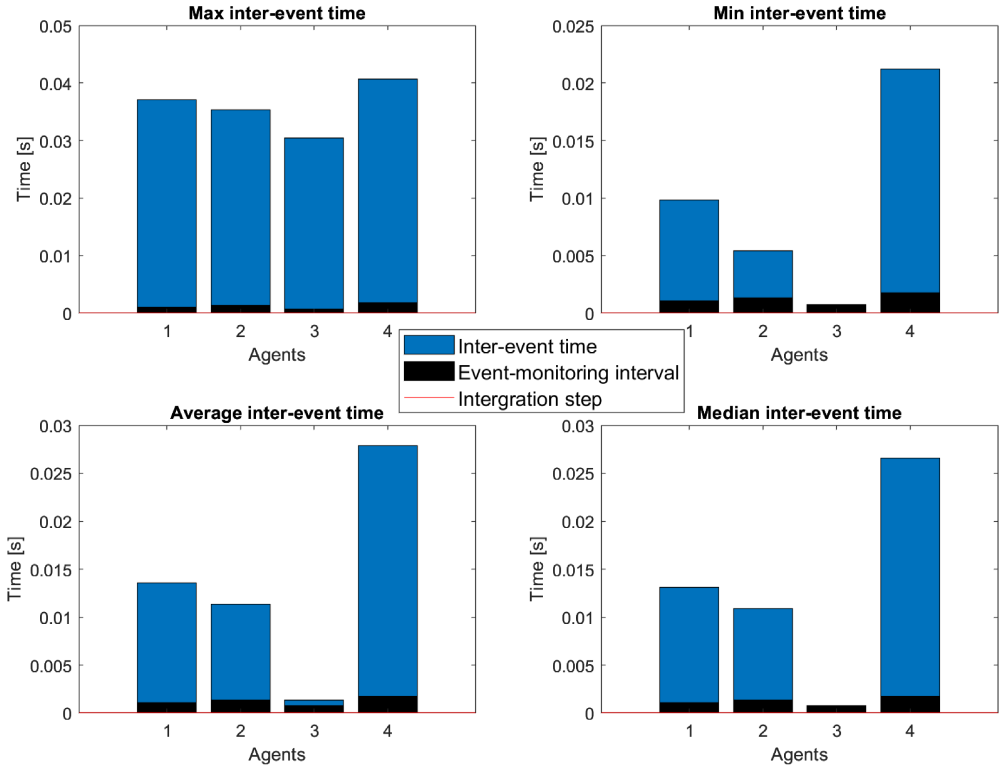

Figure 4.4: Max, min, average, and median inter-event times of LTI agents, with Theorem 2.

Similar to the numerical example involving the single-integrator MAS in Section 3.3, it can be seen through Table 4.1 that the control update frequency is significantly reduced compared to a sample-data protocol. Based on Figure 4.1, Figure 4.2, and Table 4.1, the CTETM is capable of achieving consensus faster and with less events triggered overall. The total number of events triggered and EMIs given our dynamic PETM are $9,400$ and $35,619$, respectively. Meanwhile, the CTETM triggered a total of $6,066$ events. However, comparing the sensing costs for the MAS employing the laser diode in [50], Theorem 2's PETM protocol would have consumed $90\,\text{watts} \times 100\,\text{ns} \times 35619\,\text{pulses} = 0.3206\,\text{joules}$ while $90\,\text{watts} \times 10\,\text{s} \times 4\,\text{agents} = 3600\,\text{joules}$ would have been consumed (hypothetically) with the CTETM. It can be seen that our protocol presents a total saving to sensing resources by $1.1 \times 10^6\%$ while incurring an increase to the event frequency by 150% within this simulation. In Figure 4.3, especially pronounced for agent 4, we can see the contributions of $\beta_i(\hat{z}_i^T \hat{z}_i)$ taking into effect where η_4 grows during flow, reducing the likeliness that $g_s^i < 0$ at jumps (thus, reducing the likeliness of event triggering).

4.4.2 Simulation 2

In this subsection we present the simulation results for the LTI MAS utilizing Theorem 3's PETM and maintaining the parameter selection as described in Section 4.4. We additionally select the parameters for the decaying exponential term within f_η^i, in accordance with Theorem 3 as:

$$[\delta_1^1, \delta_1^2, \delta_1^3, \delta_1^4] = [10, 20, 30, 40], \tag{4.63}$$

$$\delta_2^i = 0.5, \forall i \in \mathcal{V}. \tag{4.64}$$

Since $Q_1, \mathcal{E}_1, \mathcal{E}_2 > 0$, and $\delta_1^i, \delta_2^i > 0$, $\forall i \in \mathcal{V}$, and event-monitoring intervals are less than or equal to T^i for all time, consensus of the MAS in this simulation is guaranteed through the proof of Section 4.3. Figure 4.5 represents the state trajectories of each agent in the MAS, where the states can again be seen converging. Figure 4.6 presents the average consensus state trajectory $\bar{z}(t)$, which the MAS can be seen approaching consensus. Table 4.2 summarizes the event-trigger frequencies for both Theorem 3's PETM and the CTETM. Figure 4.3 plots the trajectories of the auxiliary PETM variable η. Figure 4.4 provides some statistical data with respect to the inter-event times for Theorem 3's PETM. Lastly, we incorporate Figures 4.9 and 4.10 to compare the state trajectories and average consensus state trajectories of the MAS, respectively, between Theorems 2 and 3's PETM.

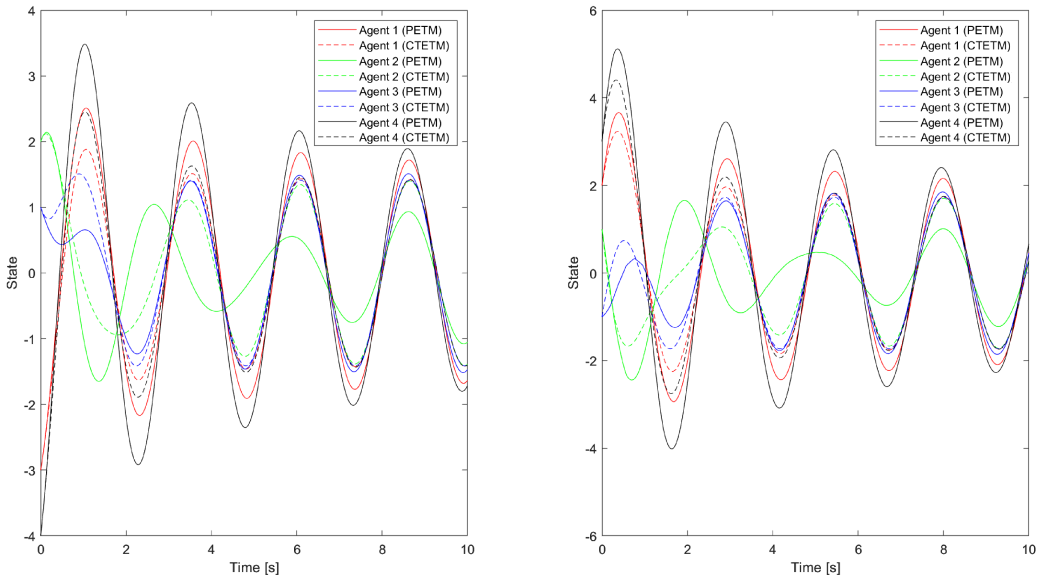

Figure 4.5: 1st (left) and 2nd (right) state trajectories of LTI agents, with Theorem 3 vs. CTETM.

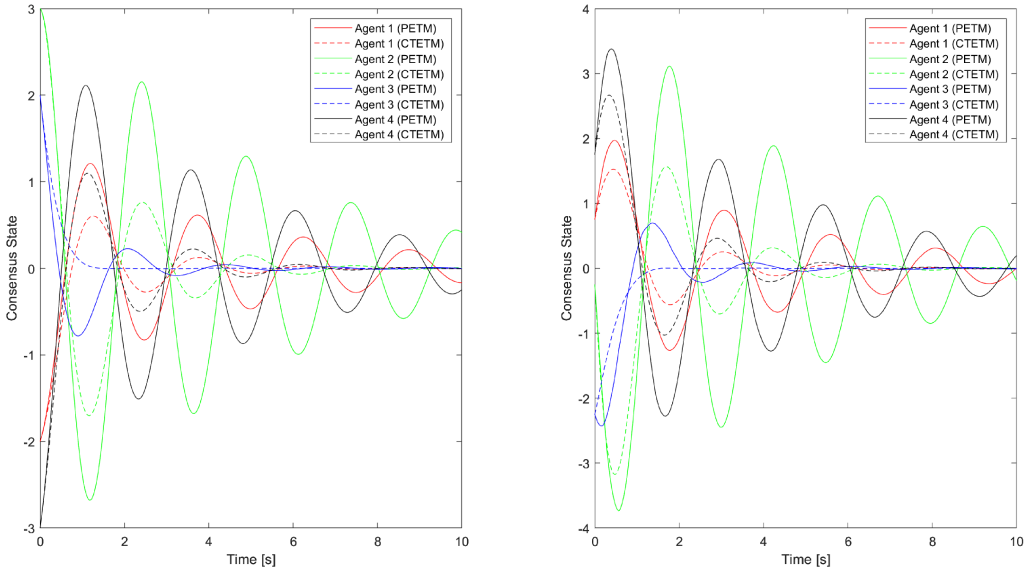

Figure 4.6: 1st (left) and 2nd (right) average consensus state trajectories of LTI agents, with Theorem 3 vs. CTETM.

Table 4.2: ETM performance comparison between dynamic PETM, according to Theorem 3, against CTETM given LTI agents.

Agents	Events Triggered (PETM)	Event Monitoring Instants (PETM)	Triggering Frequency (PETM)	Events Triggered (CTETM)
1	29	9252	0.31%	1762
2	48	7404	0.65%	2841
3	50	13282	0.37%	408
4	28	5681	0.50%	1055

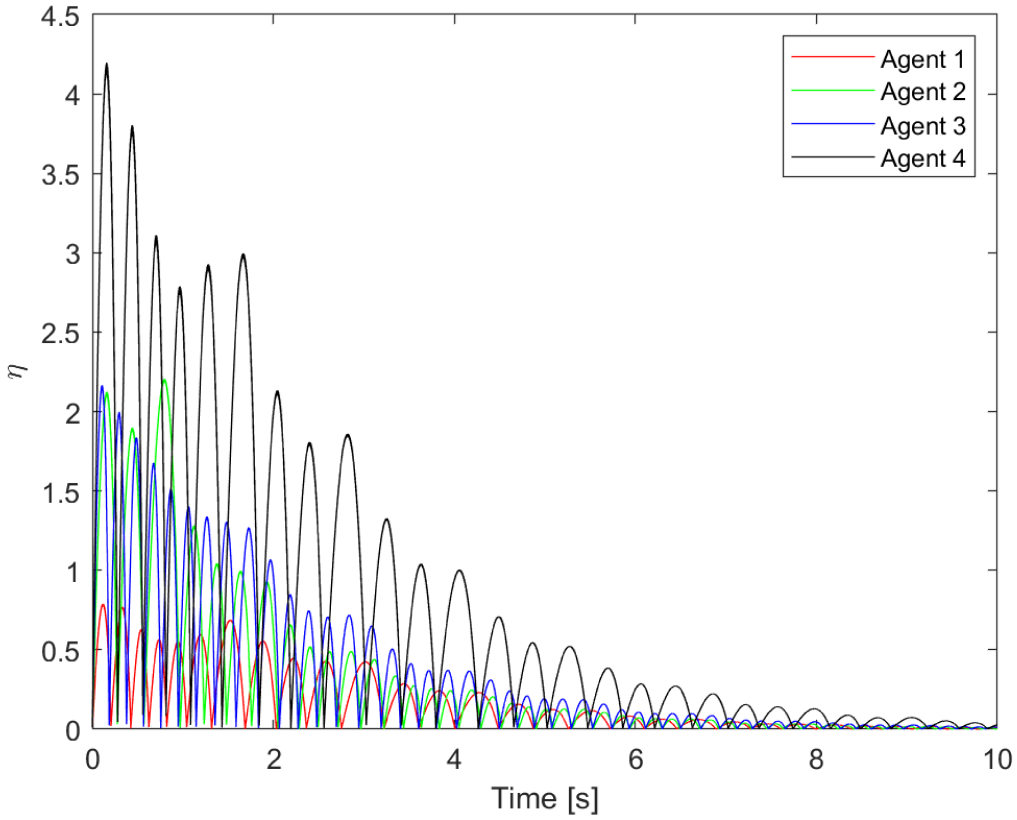

Figure 4.7: η trajectories of LTI agents, with Theorem 3.

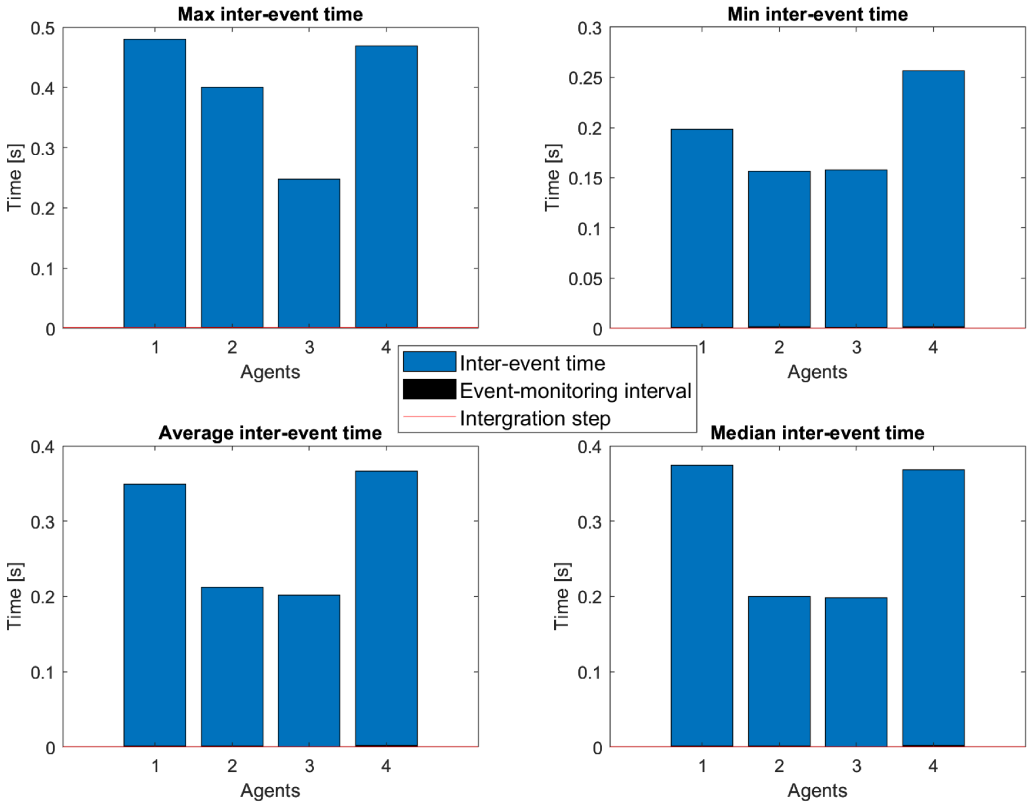

Figure 4.8: Max, min, average, and median inter-event times of LTI agents, with Theorem 3.

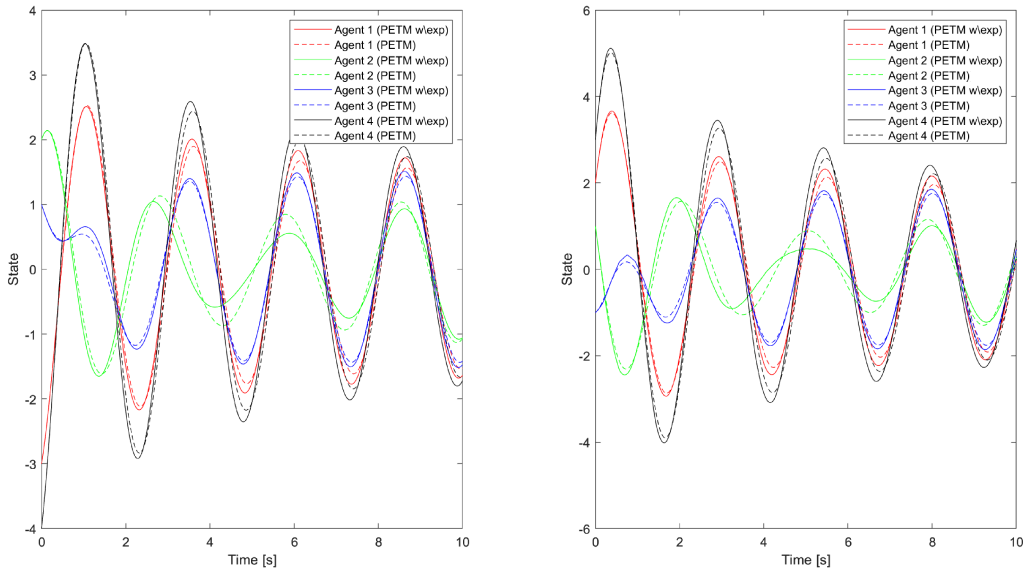

Figure 4.9: 1st (left) and 2nd (right) state trajectories of LTI agents, with Theorem 3 vs. Theorem 2.

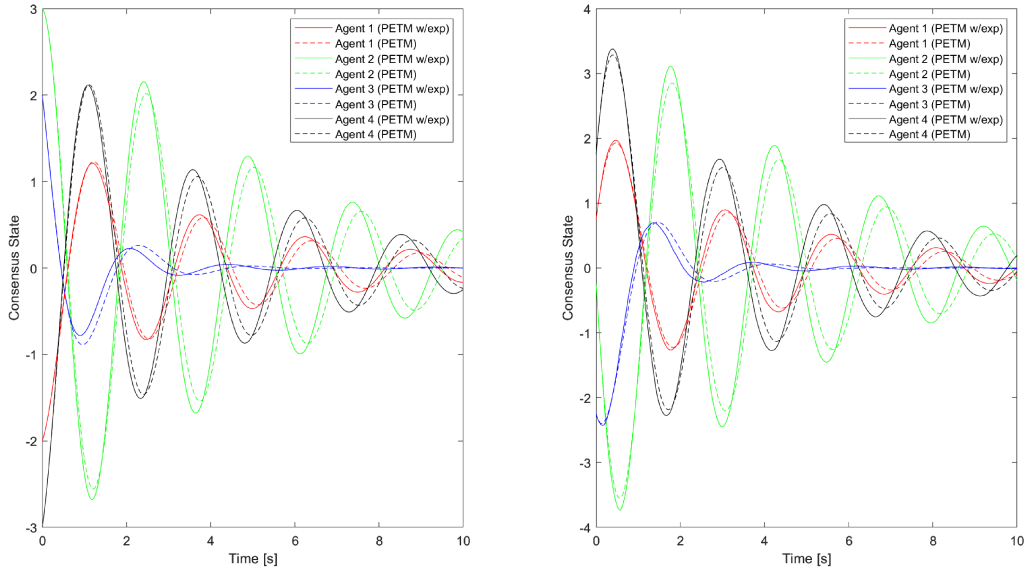

Figure 4.10: 1st (left) and 2nd (right) average consensus state trajectories of LTI agents, with Theorem 3 vs. Theorem 2.

As a result of the decaying exponential term, we see that the event frequency employing Theorem 3's PETM is significantly reduced, evident by Table 4.2. In fact, the total number of events triggered is 155 compared to $9,400$ and $6,066$ of Theorem 2's PETM and the CTETM, respectively. This reduction in events triggered is attributed to the significant growth of η during flow. Particularly, we see from the trajectory of η in Figure 4.7 (taking note of the scale on the vertical axis) that there exists a greater threshold compared to Figure 4.3 at jumps, thus reducing the likeliness that $g_s^i < 0$ at jumps. The reduction in event-frequency is also reflected in Figure 4.8 by the overall increase in inter-event times compared with Figure 4.4. As time progresses, we see that the contribution of the exponential term diminishes; thus, the PETM then becomes dominated by the contributions of $\beta_i(\hat{z}_i^T \hat{z}_i)$ in reducing event frequencies. Based on the simulation, Theorem 3's PETM proves superior in terms of both reducing sensing resource consumption and the event frequency compared to even the CTETM. Meanwhile, consensus performance as a result of Theorem 3's PETM is comparable to that of Theorem 2's, evident by Figures 4.9 and 4.10. However, the cost of Theorem 3 is that some level of feedback is sacrificed within the PETM, due to the exponential decaying term.

Chapter 5

Conclusion and Future Work

In this chapter, we conclude the research and work performed under this thesis. As closing notes, we present some potential extensions and directions for future work.

5.1 Conclusion

Motivated by the growing applications and scale of implementation of MASs, this thesis studies the consensus problem for MASs employing an event-triggered protocol. Through our literature survey, we discovered that the research gap involving distributed MAS consensus, under an undirected graph, where the agents employs RSM sensing capabilities combined with a dynamic PETM, warranted further study. Addressing the research gap, our specific contributions consist of establishing sufficient conditions on the design of the dynamic PETM such that the consensus problem is solved, and deriving an expression to pre-compute an upper bound on EMIs, individually, for each agent. To that effect, our research and main results culminated in three theorems. For each of the theorems, we modelled the MAS under the hybrid system framework and utilized the Lyapunov stability theorem to prove and guarantee consensus. The results of the three theorems are summarized as follows:

1. Theorem 1 establishes sufficient conditions for the construction and parameter selection of the dynamic PETM such that the consensus problem identified in the research gap is solved for a single-integrator MAS. We presented a modified expression, Lemma 1, to pre-compute T^i for

each agent. In the numerical example, it was evident that Theorem 1's PETM resulted in significant savings in sensing resources and triggered less events while, overall, achieving similar consensus performance as compared to the CTETM.

2. Theorem 2 extends the results of Theorem 1 from single-integrator agents to more general LTI agents by updating the sufficient conditions of the PETM to account for the A matrix. Once again, we see that Theorem 2's PETM resulted in significant sensing resource saving, but, this time, at the cost of higher event frequency while consensus performance is slower compared to the CTETM.

3. Theorem 3 modifies the construction of the dynamic PETM of Theorem 2 to provide greater design freedom in reducing event frequencies by incorporating a decaying exponential term into the CT dynamics of the PETM auxiliary variable. The exponential term potentially causes the state of the auxiliary variable to grow during flow, thus reducing the likeliness that the triggering condition is violated at jumps (thereby, reducing event frequencies). In the proof, we employed Barbalat's lemma to overcome the contribution of the exponential term in satisfying the conditions to guarantee consensus in the sense of Lyapunov. In the numerical example, for the same LTI MAS, the sensing resource consumption and the event frequency were significantly reduced with Theorem 3's PETM compared to the CTETM. Additionally, the consensus performance is similar to that of Theorem 2's PETM, though it comes at the cost of sacrificing some level of feedback within the PETM.

5.2 Future Work

Some possible extensions and future directions of the work performed within this thesis are provided below:

1. In applications, when utilizing sensors to measure the RSM, there is typically measurement noise introduced. One possible extension is to investigate the consensus performance and ETM performance when disturbance is introduced in each agent's input $u_i(t)$.

2. With digital hardware, namely, sensors or processors, there is typically quantization of information that occurs and possibly saturation. These phenomenons are exacerbated with low-bit hardware that are widely employed due to their cost-effectiveness. As such, another possible extension is to investigate the consensus performance and ETM performance when some level of quantization and saturation are considered within each agent's input $u_i(t)$.

3. As can be seen in the numerical example for the LTI MAS within this thesis, it is difficult to pre-determine where the agents will converge in consensus as it is based on initial conditions and evolution of agents' states. In other words, it would be beneficial to designers if the final consensus state can be pre-determined or dictated. One possible approach is time-varying reference (or target tracking) of a pre-determined consensus trajectory. For example, a consensus trajectory that follows a circle where the agents not only consensus with each other but consensus following this consensus trajectory.

Bibliography

[1] A. Koubâa, D. Martínez, and J. Ramiro, *Cooperative Robots and Sensor Networks*. Cham: Springer International Publishing, 2015, vol. 604.

[2] P. Shi and B. Yan, "A survey on intelligent control for multiagent systems," *IEEE Transactions on Systems, Man, and Cybernetics: Systems*, vol. 51, no. 1, pp. 161–175, 2021.

[3] Z. Meng, D. V. Dimarogonas, and K. H. Johansson, "Attitude coordinated control of multiple underactuated axisymmetric spacecraft," *IEEE Transactions on Control of Network Systems*, vol. 4, no. 4, pp. 816–825, 2017.

[4] Q. Jin, G. Wu, K. Boriboonsomsin, and M. Barth, "Advanced intersection management for connected vehicles using a multi-agent systems approach," presented at the 4$^{\text{th}}$ Intelligent Vehicles Symposium, 2012, pp. 932–937.

[5] J. Cai, C. Xiao, J. Wang, J. Feng, and H. Gong, "Adaptive event-triggered consensus of multi-agent systems with spherical polar coordinate quantization mechanism," *Physica A: Statistical Mechanics and its Applications*, vol. 627, p. 129 142, 2023.

[6] S. Knorn, Z. Chen, and R. H. Middleton, "Overview: collective control of multiagent systems," *IEEE Transactions on Control of Network Systems*, vol. 3, no. 4, pp. 334–347, 2016.

[7] R. Olfati-Saber, J. A. Fax, and R. M. Murray, "Consensus and cooperation in networked multi-agent systems," *Proceedings of the IEEE*, vol. 95, no. 1, pp. 215–233, 2007.

[8] W. Ren and R. W. Beard, *Distributed Consensus in Multi-vehicle Cooperative Control* (Communications and Control Engineering), E. D. Sontag, M. Thoma, A. Isidori, and J. H. Van Schuppen, Eds. London: Springer, 2008.

[9] R. Saber and R. Murray, "Consensus protocols for networks of dynamic agents," presented at the American Control Conference, vol. 2, 2003, pp. 951–956.

[10] A. Amirkhani and A. H. Barshooi, "Consensus in multi-agent systems: a review," *Artificial Intelligence Review*, vol. 55, no. 5, pp. 3897–3935, 2022.

[11] E. Aranda-Escolástico, M. Guinaldo, M. Miśkowicz, and S. Dormido, "Event-based control in industry practice: paving the way toward resource-efficient industrial internet of things," *IEEE Industrial Electronics Magazine*, pp. 2–11, 2023.

[12] R. Rico, J. Rico-Azagra, and M. Gil-Martinez, "Hardware and RTOS design of a flight controller for professional applications," *IEEE Access*, vol. 10, pp. 134 870–134 883, 2022.

[13] P. Tabuada, "Event-triggered real-time scheduling of stabilizing control tasks," *IEEE Transactions on Automatic Control*, vol. 52, no. 9, pp. 1680–1685, 2007.

[14] C. Nowzari and J. Cortes, "Zeno-free, distributed event-triggered communication and control for multi-agent average consensus," presented at the American Control Conference, 2014, pp. 2148–2153.

[15] C. Godsil and G. Royle, *Algebraic Graph Theory* (Graduate Texts in Mathematics). New York: Springer, 2001, vol. 207.

[16] H. Su and S. Miao, "Consensus on directed matrix-weighted networks," *IEEE Transactions on Automatic Control*, vol. 68, no. 4, pp. 2529–2535, 2023.

[17] D. V. Dimarogonas, E. Frazzoli, and K. H. Johansson, "Distributed event-triggered control for multi-agent systems," *IEEE Transactions on Automatic Control*, vol. 57, no. 5, pp. 1291–1297, 2012.

[18] Z. Chen, Q. L. Han, Y. Yan, and Z. G. Wu, "How often should one update control and estimation: review of networked triggering techniques," *Science China Information Sciences*, vol. 63, no. 5, p. 150 201, 2020.

[19] W. Hu, L. Liu, and G. Feng, "Consensus of linear multi-agent systems by distributed event-triggered strategy," *IEEE Transactions on Cybernetics*, vol. 46, no. 1, pp. 148–157, 2016.

[20] Z. G. Wu, Y. Xu, Y. J. Pan, H. Su, and Y. Tang, "Event-triggered control for consensus problem in multi-agent systems with quantized relative state measurements and external disturbance," *IEEE Transactions on Circuits and Systems I: Regular Papers*, vol. 65, no. 7, pp. 2232–2242, 2018.

[21] C. Wu, X. Zhao, W. Xia, J. Liu, and T. Başar, "L2-gain analysis for dynamic event-triggered networked control systems with packet losses and quantization," *Automatica*, vol. 129, p. 109 587, 2021.

[22] E. Garcia, Y. Cao, and D. W. Casbeer, "Decentralized event-triggered consensus with general linear dynamics," *Automatica*, vol. 50, no. 10, pp. 2633–2640, 2014.

[23] X. Meng, L. Xie, and Y. C. Soh, "Asynchronous periodic event-triggered consensus for multi-agent systems," *Automatica*, vol. 84, pp. 214–220, 2017.

[24] X. Li, Y. Tang, and H. R. Karimi, "Consensus of multi-agent systems via fully distributed event-triggered control," *Automatica*, vol. 116, pp. 108–898, 2020.

[25] C. J. Li, G. P. Liu, P. He, F. Deng, and H. Li, "Relative states-based consensus for sampled-data second-order multiagent systems with time-varying topology and delays," *IEEE Transactions on Cybernetics*, pp. 1–11, 2023.

[26] Z. Li, Z. Duan, G. Chen, and L. Huang, "Consensus of multiagent systems and synchronization of complex networks: a unified viewpoint," *IEEE Transactions on Circuits and Systems I: Regular Papers*, vol. 57, no. 1, pp. 213–224, 2010.

[27] W. P. M. H. Heemels, A. R. Teel, N. van de Wouw, and D. Nešić, "Networked control systems with communication constraints: Tradeoffs between transmission intervals, delays and performance," *IEEE Transactions on Automatic Control*, vol. 55, no. 8, pp. 1781–1796,

[28] W. Heemels, K. Johansson, and P. Tabuada, "An introduction to event-triggered and self-triggered control," presented at the 51st IEEE Conference on Decision and Control, 2012, pp. 3270–3285.

[29] C. Nowzari, E. Garcia, and J. Cortés, "Event-triggered communication and control of networked systems for multi-agent consensus," *Automatica*, vol. 105, pp. 1–27, 2019.

[30] R. K. Mishra and H. Ishii, "Average consensus in discrete-time multi-agent systems with distributed event-triggered control," presented at the European Control Conference, 2021, pp. 608–613.

[31] G. Duan, F. Xiao, and L. Wang, "Asynchronous periodic edge-event triggered control for double-integrator networks with communication time delays," *IEEE Transactions on Cybernetics*, vol. 48, no. 2, pp. 675–688, 2018.

[32] L. Xia, Q. Li, R. Song, and Y. Feng, "Dynamic asynchronous edge-based event-triggered consensus of multi-agent systems," *Knowledge-Based Systems*, vol. 272, p. 110 531, 2023.

[33] B. Luo, T. Huang, and D. Liu, "Periodic event-triggered suboptimal control with sampling period and performance analysis," *IEEE Transactions on Cybernetics*, vol. 51, no. 3, pp. 1253–1261, 2021.

[34] Q. Liu, J. Qin, and C. Yu, "Event-based multi-agent cooperative control with quantized relative state measurements," presented at the 55$^{\text{th}}$ Conference on Decision and Control, 2016, pp. 2233–2239.

[35] M. H. Dhullipalla, H. Yu, and T. Chen, "A framework for distributed control via dynamic periodic event-triggering mechanisms," *Automatica*, vol. 146, p. 110 548, 2022.

[36] K. Bansal and P. Mukhija, "Hybrid aperiodic control of distributed networked nonlinear systems," presented at the Region 10 Symposium (TENSYMP), 2019, pp. 409–414.

[37] W. Heemels and M. Donkers, "Model-based periodic event-triggered control for linear systems," *Automatica*, vol. 49, no. 3, pp. 698–711, 2013.

[38] T. Chen and B. A. Francis, *Optimal Sampled-Data Control Systems*. London: Springer, 1995.

[39] D. Nesic, A. R. Teel, and D. Carnevale, "Explicit computation of the sampling period in emulation of controllers for nonlinear sampled-data systems," *IEEE Transactions on Automatic Control*, vol. 54, no. 3, pp. 619–624, 2009.

[40] K. Bansal and P. Mukhija, "A hybrid aperiodic sampled-data strategy for distributed networked control system," presented at the 12th Asian Control Conference, 2019.

[41] H. Yu and F. Hao, "Input-to-state stability of integral-based event-triggered control for linear plants," *Automatica*, vol. 85, pp. 248–255, 2017.

[42] Q.-Q. Yang, J. Li, X. Feng, S. Wu, and F. Gao, "Event-triggered consensus for second-order multi-agent systems via asynchronous periodic sampling control approach," *International Journal of Control, Automation and Systems*, vol. 18, no. 6, pp. 1399–1411, 2020.

[43] R. Goebel, R. G. Sanfelice, and A. R. Teel, "Hybrid dynamical systems," *IEEE Control Systems*, vol. 29, no. 2, pp. 28–93, 2009.

[44] G. Zhao, C. Hua, and X. Guan, "Distributed event-triggered consensus of multiagent systems with communication delays: a hybrid system approach," *IEEE Transactions on Cybernetics*, vol. 50, no. 7, pp. 3169–3181, 2020.

[45] R. Goebel and A. Teel, "Solutions to hybrid inclusions via set and graphical convergence with stability theory applications," *Automatica*, vol. 42, no. 4, pp. 573–587,

[46] W. Li, H. Zhang, Y. Wang, and C. Liu, "Fully distributed adaptive event-triggered leaderless consensus protocol for physically interconnected multi-agent systems," presented at the Chinese Control And Decision Conference, 2020, pp. 5153–5158.

[47] H. Khalil, *Nonlinear Systems*. Upper Saddle River, NJ: Prentice Hall, 1996.

[48] A. Girard, "Dynamic triggering mechanisms for event-triggered control," *IEEE Transactions on Automatic Control*, vol. 60, no. 7, pp. 1992–1997, 2015.

[49] R. Goebel, R. G. Sanfelice, and A. R. Teel, *Hybrid Dynamical Systems: Modeling Stability, and Robustness*. New Jersey: Princeton University Press, 2012.

[50] Osram, "Nanostack Pulsed Laser Diode Array 90 W Peak Power", Technical Data Sheet, 2007.